Renewable and Sustainable Energy Reviews 119 (2020) 109582

Contents lists available at ScienceDirect

Renewable and Sustainable Energy Reviews

journal homepage: http://www.elsevier.com/locate/rser

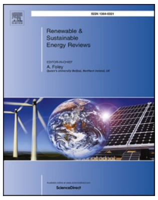

Biochar-based adsorbents for carbon dioxide capture: A critical review

Pavani Dulanja Dissanayake [a,i,1], Siming You [b,1], Avanthi Deshani Igalavithana [a], Yinfeng Xia [c], Amit Bhatnagar [d], Souradeep Gupta [e], Harn Wei Kua [e], Sumin Kim [f], Jung-Hwan Kwon [g], Daniel C.W. Tsang [h,**], Yong Sik Ok [a,j,*]

[a] *Korea Biochar Research Center, O-Jeong Eco-Resilience Institute & Division of Environmental Science and Ecological Engineering, Korea University, Seoul 02841, Republic of Korea*
[b] *School of Engineering, University of Glasgow, Glasgow, UK*
[c] *College of Water Conservancy and Environmental Engineering, Zhejiang University of Water Resources and Electric Power, Hangzhou 310018, People's Republic of China*
[d] *Department of Environmental and Biological Sciences, University of Eastern Finland, P.O. Box 1627, Kuopio FI-70211, Finland*
[e] *Department of Building, School of Design and Environment, National University of Singapore, 4 Architecture Drive, S117566, Singapore*
[f] *Department of Architecture and Architectural Engineering, Yonsei University, Seoul 03722, Republic of Korea*
[g] *Division of Environmental Science and Ecological Engineering, Korea University, Seoul 02841, Republic of Korea*
[h] *Department of Civil and Environmental Engineering, Hong Kong Polytechnic University, Hung Hom, Kowloon, Hong Kong*
[i] *Soils and Plant Nutrition Division, Coconut Research Institute, Lunuwila 61150, Sri Lanka*
[j] *Henan Province Engineering Research Center for Biomass Value-added Products, School of Forestry, Henan Agricultural University, Zhengzhou 450002, China*

ARTICLE INFO

Keywords:
Black carbon
CO_2 capture
Climate change
Engineered biochar
Greenhouse gas

ABSTRACT

Carbon dioxide (CO_2) is the main anthropogenic greenhouse gas contributing to global warming, causing tremendous impacts on the global ecosystem. Fossil fuel combustion is the main anthropogenic source of CO_2 emissions. Biochar, a porous carbonaceous material produced through the thermochemical conversion of organic materials in oxygen-depleted conditions, is emerging as a cost-effective green sorbent to maintain environmental quality by capturing CO_2. Currently, the modification of biochar using different physico-chemical processes, as well as the synthesis of biochar composites to enhance the contaminant sorption capacity, has drawn significant interest from the scientific community, which could also be used for capturing CO_2. This review summarizes and evaluates the potential of using pristine and engineered biochar as CO_2 capturing media, as well as the factors influencing the CO_2 adsorption capacity of biochar and issues related to the synthesis of biochar-based CO_2 adsorbents. The CO_2 adsorption capacity of biochar is greatly governed by physico-chemical properties of biochar such as specific surface area, microporosity, aromaticity, hydrophobicity and the presence of basic functional groups which are influenced by feedstock type and production conditions of biochar. Micropore area ($R^2 = 0.9032$, $n = 32$) and micropore volume ($R^2 = 0.8793$, $n = 32$) showed a significant positive relationship with CO_2 adsorption capacity of biochar. These properties of biochar are closely related to the type of feedstock and the thermochemical conditions of biochar production. Engineered biochar significantly increases CO_2 adsorption capacity of pristine biochar due to modification of surface properties. Despite the progress in biochar development, further studies should be conducted to develop cost-effective, sustainable biochar-based composites for use in large-scale CO_2 capture.

1. Introduction

Global warming caused by the anthropogenic emission of greenhouse gases such as carbon dioxide (CO_2), methane (CH_4), and nitrous oxide (N_2O) has become a serious environmental issue in the last few decades [1]. It has been reported that CO_2 is the main greenhouse

---

* Corresponding author. Korea Biochar Research Center, O-Jeong Eco-Resilience Institute & Division of Environmental Science and Ecological Engineering, Korea University, Seoul 02841, Republic of Korea.

** Co-corresponding author.

E-mail addresses: dan.tsang@polyu.edu.hk (D.C.W. Tsang), yongsikok@korea.ac.kr (Y.S. Ok).

[1] The authors contributed equally to the paper.

https://doi.org/10.1016/j.rser.2019.109582
Received 19 April 2019; Received in revised form 25 October 2019; Accepted 8 November 2019

gas responsible for global warming [2]. Since 1750, the atmospheric CO_2 concentration has increased reaching a level of 410 ppm at present [2]. The International Panel on Climate Change (IPCC) has predicted that the CO_2 concentration will reach 570 ppm by 2100, leading to a mean temperature increase of 1.9 °C [3]. This would lead to tremendous impacts on the terrestrial environment, causing heavy droughts, changes in rainfall patterns, extreme heat waves, melting of glaciers, and rising sea levels [4]. Thus, it is essential to develop sustainable methods for capturing and storing CO_2 to reduce CO_2 emissions and combat global warming, as underlined by the fifth assessment report of the IPCC [3].

CO_2 capture technologies can be categorized into three groups: pre-combustion CO_2 capture, post-combustion CO_2 capture, and oxy-fuel combustion [5]. In pre-combustion CO_2 capture, H_2 and CO_2 are produced through the gasification of fossil fuel in a water-gas-shift reactor, and H_2 is used for energy generation, whereas CO_2 is captured before the combustion of the fossil fuel [4]. During post-combustion, CO_2 is separated and captured from the effluent gas produced during fossil fuel combustion [4]. Oxy-fuel combustion is the process of burning fuel with pure O_2 instead of air as the primary oxidant [4]. The nitrogen-free and oxygen-rich environment results in a more concentrated CO_2 stream in the final flue gas, leading to easier purification [6].

Post-combustion CO_2 capture technologies have gained more interest because of their low technological risk and better compatibility with current gas emission control systems [17]. Specifically, solvent absorption, adsorption with solid sorbents, membrane separation, and cryogenic separation are commonly used for post-combustion CO_2 capture [8]. Adsorption is considered the best technique because of its low energy consumption, the ability to use this technology at a wide range of temperatures and pressures, and the ease of adsorbent regeneration, without producing any unfavorable byproducts [9]. Various adsorbents such as zeolite, mesoporous carbon, engineered carbon nanomaterials, and activated carbon have been studied for use as CO_2 adsorbents over past few years [10]. Even though these materials show good adsorption performance for capturing CO_2, their use on a large scale is associated with some drawbacks such as adsorption competition and high cost [11].

Biochar is a porous carbonaceous material produced through the thermochemical conversion of organic material in oxygen-depleted conditions which is also known as pyrolysis [12] and at moderate temperatures usually below 700 °C [13,14]. Recently, biochar has been used for various environmental applications including soil quality improvement [15], removal of emerging contaminants in soil [16,17] and water [18], mitigation of greenhouse gas emissions [19], and energy production [20,21]. The potential for using biochar for various environmental applications varies with the properties of the biochar, which are affected by the feedstock type and production conditions [22,23]. As biochar can be produced using abundant biomass and waste, such as crop residues [24,25], wood waste [24,26], animal manure, food waste [27], municipal solid waste [28], and sewage sludge [29] it is regarded as an environmentally friendly material for capturing CO_2 [30,31]. In addition, use of waste-derived biochar for CO_2 capture will facilitate sustainable waste management. Activated carbon is being widely used as an adsorbent for removal of various environmental contaminants. Despite of its excellent adsorption capacity, high cost and difficulties in regeneration limit the use of activated carbon as an effective adsorbent [32]. The break-even price of biochar is approximately one sixth of that of activated carbon [13]. In general, activated carbon is produced under higher temperature (800–1000 °C) [12] and an additional activation process is crucial in activated carbon production incurring more-energy consumption and a higher cost compared to biochar which is usually produced at a lower temperature ($<$700 °C) and activation is unnecessary for biochar production [13,33]. Moreover, the average energy demand for activated carbon production (97 MJ/kg) is significantly higher than that of biochar (6.1 MJ/kg) [34]. Biochar production from waste biomass can benefit both carbon abatement and sustainable management. Carbon dioxide in the atmosphere is first removed by green plants through photosynthesis part of which will then bound to the final carbonaceous structure of biochar without liberating for hundreds of years [14,19]. The economic feasibility of biochar production is highly contingent up the cost of feedstock, and waste biomass serves as economic feedstocks for biochar production in view of its relatively low cost or even income generating potential in the form of tipping fees [35]. Hence, waste based biochar production is considered as a potential sustainable process.

At present, there is much interest in the scientific community in enhancing the adsorption capacity of biochar by modifying its structure and surface properties [36]. The product that is obtained by modification of pristine biochar (unmodified normal biochar) through physical, chemical and biological methods to improve its physical, chemical and biological properties is known as engineered biochar [37]. Because of the high surface area and porous structure of engineered biochar, it can be used as a potent CO_2 adsorbent [30]. This review aims to evaluate and summarize the potential of using pristine and engineered biochar as a CO_2 capturing medium. It also discusses the factors influencing the CO_2 adsorption capacity of biochar as well as relevant issues related to the synthesis of biochar-based CO_2 adsorbents.

2. Biochar as a potential CO_2 adsorbent

Biochar is an eco-friendly adsorbent that is produced from natural biomass or agricultural waste. Biochar is nearly ten times cheaper than other CO_2 adsorbents because of the wide availability of biomass [38]. Raw biochar exhibits a low adsorption capacity towards CO_2, but modified biochar has shown enhanced CO_2 adsorption in many studies. Several modification methods have been tested and applied with varying degrees of success (Section 4).

Many studies have suggested that the introduction of basic nitrogen functional groups would enhance the basic sites on biochar and increase the uptake of acidic CO_2 [39]. Considering that the amine modification of biochar results in a superior surface chemistry for the uptake of CO_2, chicken manure was converted to biochar by pyrolysis at 450 °C for 1 h, followed by chemical treatment with HNO_3 and ammonia gas for 1 h at 450 °C [39]. The modified biochar was further treated with sodium α-L-gulopyranuronate to produce compact beads for easy sorting after the process. The biochar beads had a specific surface area of 328.6 m^2/g with high adsorption capacity. To increase the nitrogen content and the micro-porosity of the adsorbent, Zhang et al. [40] investigated the high-temperature ammonia treatment of biochar with CO_2 activation.In this study, the micropore volume of the biochar was correlated with the CO_2 adsorption capacity. Studies investigating the CO_2 and NH_3 activation of biochar for CO_2 adsorption have been conducted with cotton stalk biochar by Xiong et al. [41]. The maximum specific surface area of the CO_2-modified biochar (610.04 m^2/g) was higher than that of the NH_3-modified biochar (348.56 m^2/g) at 800 °C. The CO_2 uptake capacity of CO_2-modified biochar was 100 mg/g (at 20 °C).

The performance of virgin and amine-modified biochar (coconut shell) has also been assessed [42]. It was reported that amine-modified biochar pyrolyzed at 800 °C presented the highest adsorption of CO_2 that was reported to be 35.57 mg/g at 30 °C. The amine treatment of biochar was important because it increased the number of nitrogen-containing functional groups and basicity, which increased the overall CO_2 adsorption. In addition, the potential of untreated and amine-treated sawdust biochar was also evaluated for CO_2 adsorption [43]. In contrast to other studies, this study showed lower CO_2 adsorption in the modified biochar than the unmodified biochar. The reason for the lower CO_2 uptake by the modified biochar was attributed to the incorporation of nitrogen functional groups on the carbon surface, which resulted in the pore obstruction of the amine film and inhibited the CO_2 uptake. Three different ammoxidation methods were studied by Liu et al. [44] to prepare biochar from coffee grounds: (i) dispersion of carbonized carbon from the coffee grounds in alcohol containing 3-aminopropyltrimethoxysilane (APTES) followed by refluxing and washing,

(ii) dispersion of carbonized carbon from coffee grounds in HCl and treatment by the polycondensation of $C_6H_5NH_2$ by $K_2Cr_2O_7$ in an ice bath for 6 h followed by washing and drying, and (iii) dissolution of carbonized carbon from coffee grounds in H_2O via sonication, addition of melamine into the solution, hydrothermal treatment at 160 °C for 24 h, and, finally, drying at 60 °C. The prepared products were chemically activated with KOH and heated to 400 °C for 1 h, followed by ramping to 600 °C for a further hour. The adsorption capacity was 89.78–117.51 mg/g. The adsorbent prepared by method (iii) and after the KOH treatment exhibited the maximum CO_2 removal (117.51 mg/g) compared to the other adsorbents prepared in this study. A possible reason for this observation is the well-developed microporous structure, high nitrogen doping, and creation of active sites for adsorption in this particular adsorbent (i.e., that prepared via method (iii)).

A two-stage biochar activation process for removal of CO_2 has been reported recently based on ultrasound treatment and amine functionalization [38]. In this process, pinewood-derived biochar was first physically activated by 30-s sonication at ambient temperature. The authors stressed the need for ultrasound treatment because it resulted in the exfoliation and breaking up of the irregular graphitic layers of the biochar, which resulted in the formation of new micropores. As a result, the porosity and permeability of the biochar were increased, resulting in a higher CO_2 uptake. In the second step, tetraethylenepentamine (TEPA) was used to functionalize the biochar. The adsorption capacity of the biochar modified with ultrasonic treatment followed by TEPA (2.79 mmol/g) was more than nine times more efficient than the untreated biochar [38].

Although the pyrolysis method has been widely studied, some researchers have raised concerns about this method because of the high costs associated with the equipment and energy usage. To search for a cheaper, quicker, and more efficient pyrolysis method, Huang et al. [45] considered using microwave pyrolysis to produce biochar. In their study, biochar was prepared from rice straw by microwave pyrolysis (200 W and 300 °C). The CO_2 removal capacity was found to be up to 80 mg/g at 20 °C, and a correlation between the CO_2 removal and the specific surface area was reported. Microwave pyrolysis was suggested to be a better approach than conventional pyrolysis because of its advantages, energy recovery, and zero carbon emissions.

Xu et al. [46] considered that the presence of alkali or alkali earth metals in the biochar was important for the sorption of the acidic CO_2 molecule. Biochars were developed from sewage sludge, wheat straw, and pig manure by, pyrolyzed at 500 °C for 4 h and tested for CO_2 adsorption. The removal of CO_2 was suggested to be induced by mineralogical reactions because minerals such as magnesium, calcium, iron, and potassium were present in the biochar. It was reported that $Fe(OH)_2CO_3$ was formed in sewage sludge biochar by the transformation of FeOOH after the sorption of CO_2, whereas $K_2Ca(CO_3)_2$ and $CaMg(CO_3)_2$ were the transformation products in pig manure biochar after CO_2 sorption. The reaction between adsorbed CO_2 and calcium carbonate ($CaCO_3$) resulted in the formation of $Ca(HCO_3)_2$ in the case of wheat straw biochar. The prepared biochars show considerably high sorption efficacy for CO_2 removal (18.2–34.4 mg/g at 25 °C). Guo et al. [5] used zinc chloride as a catalyst to synthesize biochar from the pyrolysis of roasted peanut shell waste. The developed biochar had a large surface area (1087 m^2/g). The capacity for CO_2 adsorption was found to increase with increasing gas pressure and decreasing temperature. The CO_2 capturing capacity of the prepared biochar at 100 kPa was reported to be 3.8 mmol/g at 273 K and 2.2 mmol/g at 298 K.

Single-step pyrolysis at various temperatures (500, 700, and 900 °C) was used to prepare biochars from walnut shells under a N_2 atmosphere [47]. The biochar prepared at 900 °C had a high specific surface area (397.015 m^2/g) and high microporosity (0.159 cm^3/g). Metal impregnation was done followed by heat treatment with nitrogen. For metal impregnation, metal nitrate salts of sodium, magnesium, calcium, nickel, iron, and aluminum were selected. It was reported that the addition of basic sites (induced by metal impregnation) on the surface of biochar improved the capturing of CO_2. The performance of the metal-impregnated biochar followed the order: magnesium > aluminum > iron > nickel > calcium > raw biochar > sodium. The magnesium-loaded biochar exhibited a higher CO_2 uptake (82.0 mg/g) than the virgin biochar (72.6 mg/g) at 25 °C and 1 atm. The improved performance of the modified biochar attributed to combined physical and chemical effects.

Sugarcane bagasse and hickory wood were pyrolyzed at three different temperatures (300, 450, and 600 °C) under a N_2 atmosphere for the production of biochar for CO_2 removal [48]. The CO_2 adsorption capacities of the prepared biochars were found to be in the range of 34.48–73.55 mg/g at 25 °C and 11.15–43.67 mg/g at 75 °C. The larger surface area of the biochars and the presence of nitrogen-containing groups on the biochar surface was suggested to contribute toward the CO_2 capture. The biochar prepared from bagasse samples possessed a larger number of nitrogen-containg functional groups than the hickory samples and, consequently, exhibited better CO_2 removal. Creamer et al. [49] hypothesized that basic metal oxyhydroxides can easily interact with acidic CO_2 when the polar surfaces are in contact. To test this hypothesis, the authors prepared metal-oxyhydroxide–biochar composites and assessed them for CO_2 adsorption. Raw cottonwood was used to prepare the biochar, and the biochar was treated with the chloride salts of three metals (Al, Fe, and Mg). The mixture (cottonwood in metal salt) was pyrolyzed at 600 °C under a nitrogen atmosphere for 3 h. It was found that, in comparison with the raw biochar (58 mg/g), the metal-modified biochars displayed higher CO_2 adsorption, i.e., 27–63 mg/g for Mg biochar, 54–67 mg/g for Fe biochar, and 63–71 mg/g for Al biochar.

Single-step activation of biomass (almond shells and olive stones) in air at 400–500 °C and at a low oxygen content (3–5%) in the activating gas at high temperatures (500–650 °C) has also been reported [50]. Samples that were activated at 650 °C showed the highest CO_2 adsorption capacity. The almond-shell-based biochars exhibited a CO_2 removal of up to 2.1 mmol/g at 25 °C and 0.7 mmol/g at 100 °C. Four types of feedstocks, namely soybean stover, perilla leaf, Japanese oak, and Korean oak, were used to prepare different types of biochars [51]. The powdered biomass was pyrolyzed at 700 °C, and the Korean oak and Japanese oak biochars were produced at 400 and 500 °C, respectively. The efficiency of the prepared biochars for CO_2 adsorption was found to decrease in the order Perilla leaf (2.312 mmol/g) > Korean oak (0.597 mmol/g) > Japanese oak (0.379 mmol/g) > soybean stover (0.707 mmol/g), and this was related to the nitrogen contents of these biochars. In addition to the above-mentioned studies, other researchers have also investigated biochars for CO_2 adsorption [52,53].

3. Biochar properties influencing CO_2 adsorption

The CO_2 adsorption capacity of biochar, which is the amount of CO_2 adsorbed per unit weight of biochar, mainly depends on the physicochemical properties of the biochar, such as the surface area, pore size, pore volume, basicity of biochar surface, presence of surface functional groups, presence of alkali and alkali earth metals, hydrophobicity, polarity, and aromaticity [54]. These physical and chemical properties of biochar are closely related to the type of feedstock used and the thermochemical conditions of biochar production [55,56]. Table 1 summarizes the effects of feedstock type and pyrolysis conditions on the properties of the biochar.

3.1. Physical properties of biochar

Carbon dioxide adsorption occurs through van der Waals forces between gas molecules and the solid phase (biochar), which is associated with the specific surface area, pore size, and pore volume of the biochar [57].

Table 1
Effect of feedstock and pyrolysis conditions on the biochar properties

Type of feedstock	Pyrolysis conditions	C (%)	H (%)	O (%)	N (%)	Surface area (BET) (m^2/g)	Pore diameter (nm)	Pore volume (cm^3/g)	Reference
Vegetable waste	200 °C for 2 h	52.89	6.9	36.02	4.2	0.36	2.59	43.24	[58]
Vegetable waste	500 °C for 2 h	83.85	2.7	9.73	3.71	50.26	3.22	54.61	[58]
Pine cone	200 °C for 2 h	69.74	2.13	27.09	1.03	0.47	2.38	45.13	[58]
Pine cone	500 °C for 2 h	74.64	2.62	20.94	1.81	192.97	10.2	2.44	[58]
Pitch pine wood chips	300 °C fast pyrolysis	63.9	5.4	30.4	0.3	2.9	N/A	N/A	[59]
Pitch pine wood chips	400 °C fast pyrolysis	70.7	3.4	25.5	0.4	4.8	N/A	N/A	[59]
Pitch pine wood chips	500 °C fast pyrolysis	90.5	2.5	6.7	0.3	175.4	N/A	N/A	[59]
Rubber wood sawdust	300 °C for 1-h	N/A	N/A	N/A	N/A	1.8	7.4	0.0032	[60]
Rubber wood sawdust	400 °C for 1 h	N/A	N/A	N/A	N/A	1.4	9.6	0.0034	[60]
Rubber wood sawdust	500 °C for 1 h	N/A	N/A	N/A	N/A	2.2	11	0.0061	[60]
Rubber wood sawdust	600 °C for 1 h	N/A	N/A	N/A	N/A	2.7	11.8	0.008	[60]
Rubber wood sawdust	700 °C for 1 h	N/A	N/A	N/A	N/A	2.3	15.8	0.0089	[60]
Rubber wood sawdust	300 °C for 3 h	N/A	N/A	N/A	N/A	1.9	7.0	0.0034	[60]
Rubber wood sawdust	400 °C for 3 h	N/A	N/A	N/A	N/A	2.1	12.4	0.0066	[60]
Rubber wood sawdust	500 °C for 3 h	N/A	N/A	N/A	N/A	2	12.7	0.0064	[60]
Rubber wood sawdust	600 °C for 3 h	N/A	N/A	N/A	N/A	1.9	13	0.0063	[60]
Rubber wood sawdust	700 °C for 3 h	N/A	N/A	N/A	N/A	5.5	7.0	0.0097	[60]
Wheat straw	400 °C for 1.5 h	57.8	3.2	21.6	1.5	10	4.6	0.012	[61]
Wheat straw	500 °C for 1.5 h	70.3	2.9	17.7	1.4	111	3.3	0.09	[61]
Wheat straw	600 °C for 1.5 h	73.4	2.1	14.9	1.4	177	2.5	0.11	[61]
Wheat straw	700 °C for 1.5 h	73.9	1.3	14.6	1.2	107	2.2	0.058	[61]
Corn straw	400 °C for 1.5 h	56.1	4.3	22	2.4	4	8.1	0.008	[61]
Corn straw	500 °C for 1.5 h	58	2.7	21.5	2.3	6	2.1	0.012	[61]
Corn straw	600 °C for 1.5 h	58.6	2	18.7	2	7	6.3	0.012	[61]
Corn straw	700 °C for 1.5 h	59.5	1.5	16.6	1.6	3	8.2	0.006	[61]
Peanut shell	400 °C for 1.5 h	58.4	3.5	21	1.8	5	5.2	0.007	[61]
Peanut shell	500 °C for 1.5 h	64.5	2.8	18.5	1.7	28	3.2	0.022	[61]
Peanut shell	600 °C for 1.5 h	71.9	2	15	1.6	195	2.4	0.11	[61]
Peanut shell	700 °C for 1.5 h	74.4	1.4	14.2	1.4	49	2.7	0.033	[61]
Wood	850 °C for 3 h	84.5	1.0	N/A	0.5	172	N/A	0.121	[62]
Wood chip (70%) + chicken manure (30%)	850 °C for 3 h	70.7	2.1	N/A	0.7	342	N/A	0.224	[62]
Yak manure	300 °C for 3 h	41.6	1.9	27.4	3.2	3.6	11.3	N/A	[63]
Yak manure	500 °C for 3 h	41.3	1.7	24.4	3.0	17.3	7.5	4.4	[63]
Yak manure	700 °C for 3 h	41.2	1.4	20.7	2.7	82.9	3.6	52.8	[63]
Sewage sludge	500 °C for 4 h	29.1	1.56	N/A	3.34	10.12	N/A	0.022	[46]
Pig manure	500 °C for 4 h	47.7	1.91	N/A	2.49	31.57	N/A	0.044	[46]
wheat straw	500 °C for 4 h	60.5	2.31	N/A	0.97	20.2	N/A	0.041	[46]
Rice straw	300 °C for 1.5 h	N/A	N/A	N/A	N/A	3.35	151.3	0.127	[64]
Rice straw	500 °C for 1.5 h	N/A	N/A	N/A	N/A	7.47	108.1	0.0202	[64]
Rice straw	700 °C for 1.5 h	N/A	N/A	N/A	N/A	32.9	59.2	0.0486	[64]
Pig manure	300 °C for 1.5 h	N/A	N/A	N/A	N/A	3.32	229.9	0.0191	[64]
Pig manure	500 °C for 1.5 h	N/A	N/A	N/A	N/A	6.3	184.5	0.0291	[64]
Pig manure	700 °C for 1.5 h	N/A	N/A	N/A	N/A	20.5	88.4	0.0454	[64]
Rice straw (hydrochar)	300 °C for 1.5 h	N/A	N/A	N/A	N/A	2.57	314.1	0.0202	[64]
Rice straw (hydrochar)	700 °C for 1.5 h	N/A	N/A	N/A	N/A	2.94	174.3	0.0128	[64]
Pig manure (hydrochar)	300 °C for 1.5 h	N/A	N/A	N/A	N/A	15.5	233.5	0.0907	[64]
Pig manure (hydrochar)	500 °C for 1.5 h	N/A	N/A	N/A	N/A	15.6	310.6	0.1212	[64]
Pig manure (hydrochar)	700 °C for 1.5 h	N/A	N/A	N/A	N/A	10.7	272.7	0.0728	[64]

3.1.1. Specific surface area

The specific surface area of biochar can be defined as the ratio between the total surface area and the total mass of the biochar [65]. Several studies have assessed the effects of the specific surface area of biochar on its capacity of CO_2 adsorption [46]. A positive relationship ($R^2 = 0.6475$, $n = 16$) can be seen between the specific surface area and the CO_2 adsorption capacity of biochar (Fig. 1a). A larger surface area provides more active sites for CO_2 adsorption through physical adsorption; thus, a higher biochar surface area leads to a correspondingly larger adsorption capacity [10].

The specific surface area of biochar is strongly related to the carbon content of the material, which may vary depending on the feedstock [65, 68]. However, high mineral content can reduce the specific surface area by blocking the pores on the biochar surface [69]. The Brunauer–Emmett–Teller (BET) specific surface area of corn-straw-derived biochar is lower than that of the biochars derived from peanut shell and wheat straw, suggesting that this difference can be attributed to the different lignin, cellulose, and hemicellulose contents of the feedstock, which may also contribute to different decomposition rates (Fig. 2a) [61]. Biochar produced from plant materials such as corn stove, oak wood, and pine needles showed significantly higher surface areas than that of the biochar produced from animal litter such as swine manure and biosolid waste (Table 1) [18,55]. Nevertheless, a study conducted with 100% wood-derived biochar and that prepared form 70% wood +30% chicken manure showed BET surface areas of 172 and 342 m^2/g, respectively, which could be attributed to the feedstock (Table 1) [62]. In general, wood chips are larger than chicken manure granules and wood chips have a higher fixed carbon content than chicken manure (Fig. 2b), which may cause a lower burn off rate, thus contributing to a lower surface area and porosity [62].

The surface area of the biochar increases with increasing pyrolysis temperature and residence time, possibly because of the release of volatile matter, which increases the pore volume [18]. For instance, increasing temperature from 200 °C to 500 °C in biochar produced with

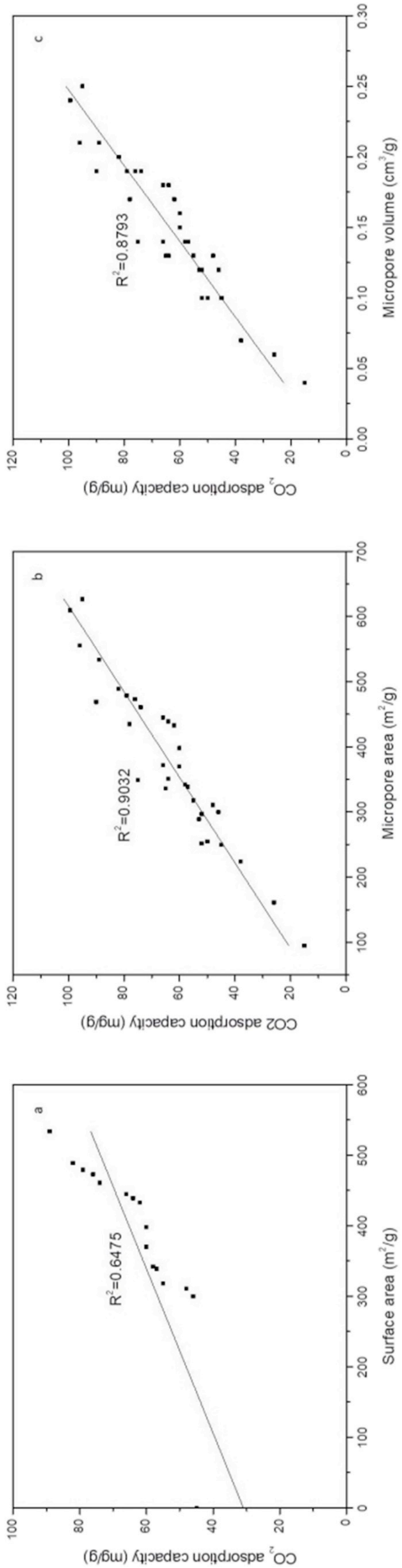

Fig. 1. Relationship between the (a) specific surface area, (b) micropore area, (c) micropore volume, and CO_2 adsorption capacity of biochar (Data was obtained from Refs. [66,67]).

vegetable waste and pine cone enhanced the surface area from 0.36 to 50.26 and 0.47–192.97 m^2/g respectively (Table 1) [58]. The mobile matter content was reduced from 56.44 to 12.43 and 62.35 to 10.01% respectively when the temperature was increased from 200 °C to 500 °C in biochar produced with vegetable waste and pine cone (Fig. 2c) [58]. This suggested that release of mobile matter would open up the pores in biochar matrix enhancing surface area. In addition, increase in the temperature from 300 to 500 °C was found to increase the specific surface area of pitch pine wood biochar from 2.9 to 175.4 m^2/g [59]. Moreover, a study conducted with wheat straw, corn straw, and peanut shell biochars revealed that the surface area of the biochar increased substantially from 300 to 600 °C, whereas a reduction was observed at 700 °C irrespective of the feedstock, suggesting the loss of H and O-containing functional groups, whereas aliphatic alkyl CH_2, aromatic CO, ester C_5O, and OH groups serve to increase the surface area at 600 °C [61,70]. A significant increase in the BET surface area of rubber wood sawdust biochar was observed at 700 °C after a residence time of 3 h [60]. It was suggested that the partially carbonized reactants may lower the surface area at lower temperatures, and the high temperature (700 °C) led to the release of a higher amount of volatile organic compounds, thus creating more pores [60].

3.1.2. *Total pore volume and pore size*

The pore volume and pore size also play a vital role in CO_2 adsorption. The release of volatile organic matter from the polymeric backbone of the feedstock causes the formation of porous structures in biochar, and a larger total pore volume provides more active sites for interaction between CO_2 and the biochar [65,79]. Per the pore size classification of the International Union of Pure and Applied Chemistry, pores with a diameter greater than 50 nm are categorized as macropores, those with a diameter between 2 and 50 nm are mesopores, and those with a diameter of less than 2 nm are micropores [65]. Generally, the CO_2 capture capacity of porous carbon strongly depends on the presence of micropores with a diameter of less than 1 nm [80,81]. Nevertheless, studies have revealed that pores with a diameter of 0.5 nm or less contribute significantly to CO_2 adsorption at low partial pressures, whereas pores with a diameter smaller than 0.8 nm make a higher contribution to CO_2 uptake at 1 bar [82]. The CO_2 adsorption capacity has a stronger correlation with the micropore surface area ($R^2 = 0.9032$, $n = 32$, Fig. 1b) than the BET surface area ($R^2 = 0.6475$, $n = 16$, Fig. 1a), suggesting that the micropore structure of the biochar significantly affects the CO_2 adsorption capacity [67].

A study conducted to assess the effect of the pyrolysis temperature on the pore volume showed that there was an increase in the micropore volume and the total pore volume of the biochar as the temperature increased from 400 to 500 °C and a reverse trend is observed when the temperature was increased above 500 °C (Table 1, Fig. 2d) [83]. When the temperature is higher than 500 °C, the coalescence of neighboring pores can widen the pores while reducing the pore volume [83]. Furthermore, even during modification of biochar using different compounds, the micropore volume and surface area of the micropores increase with increasing modification temperature but begin to decrease from 800 °C because of the coalescence of micropores and increase in mesopores and macropores [41,67].

Anglin et al. [83] also observed a reduction in pore volume with the increase of heating rate from 10 to 50 °C/min. When the heating rate of the process is low, pyrolysis products/volatile organic matter has enough time to diffuse from the biochar particles. Nevertheless, with the increase of heating rate, the time for discharging volatile organic matter reduces resulting in the accumulation of volatiles within and between particles blocking the pore entrance [83].

3.2. *Chemical properties of biochar*

The adsorption of CO_2 onto the biochar surface is also affected by the chemical properties of the biochar such as alkalinity, mineral

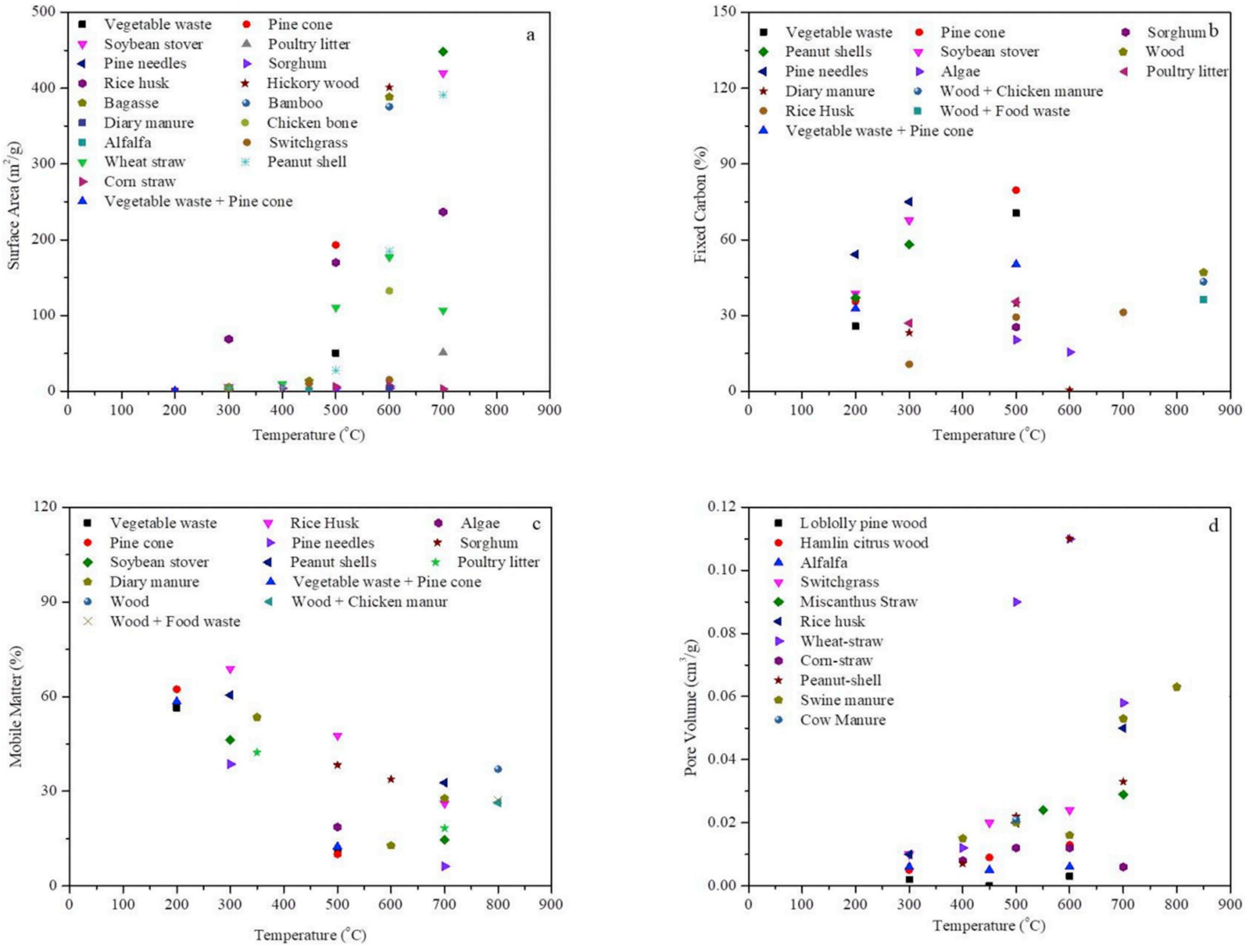

Fig. 2. Variation of (a) surface area, (b) fixed carbon content, (c) mobile matter content and (d) pore volume of biochar produced from different feedstock types under different pyrolysis temperatures (Data was obtained from Refs. [27,58,61,71–78]).

composition, presence of surface functional groups, hydrophobicity, and non-polarity [46,84]. The CO_2 adsorption capacity of biochar can be enhanced by increasing the alkalinity of the biochar surface [47].

3.2.1. *Basic functional groups*

Basic surface functional groups play an important role in the CO_2 adsorption of biochar because of their contribution to surface basicity, which enhances the affinity of the biochar for CO_2 [85]. Nitrogen-containing functional groups (e.g., amide, imide, pyridinic, pyrrolic, and lactam groups) are the contributors to the surface basicity of biochar. They can be introduced to the biochar surface through reaction with different *N*-containing reagents such as ammonia, amines, and nitric acid or by the activation of biochar with nitrogen-containing precursors (a precursor is a compound that participates in a chemical reaction while producing another compound), such as melamine or polyacrylonitrile [5,86]. The Fourier-transform infrared spectroscopy (FTIR) spectrum of ammonia-modified biochar shows C = N (1745–1586 cm^{-1}) and C–N (1056 cm^{-1}) stretches corresponding to *N*-containing functional groups [57]. Moreover, the authors observed the highest CO_2 adsorption capacity (39.37 mg/g) in the ammonia-modified biochar [57]. In addition, some oxygen-containing functional groups such as ketones, pyrones, and chromenes also contribute to the surface basicity [54]. Xing et al. [87] suggested that the basicity of *N*-containing functional groups is very weak compared to that of organic amines, but this has rarely been studied. Unlike the acid–base interaction between CO_2 and the biochar surface, there is evidence that the presence of oxygen-containing acidic functional groups such as hydroxyl groups, carboxyl groups, and carbonyl groups also increase CO_2 adsorption on carbonaceous surfaces by facilitating hydrogen bonding between the CO_2 molecules and the carbon surface [87,88].

3.2.2. *Alkaline and alkaline earth metals*

The presence of alkali metals and alkaline earth metals (e.g., Na, K, Ca, Mg, and Li) can enhance the formation of basic sites with a strong affinity for CO_2, which has an acidic nature [46]. Thus, the presence of alkaline metals and alkaline earth metals may enhance the CO_2 adsorption capacity of biochar. For instance, when biochar was loaded with $Mg(NO_3)_2$, MgO was formed when the temperature was above 400 °C which facilitated CO_2 adsorption through the interaction between CO_2 and O_2 [47]. However, the reaction between O_2 and CO_2 forms a monolayer of magnesium carbonate ($MgCO_3$) on the surface which limits the further reaction between MgO and CO_2 [89]. Additionally, decrease in the specific surface area and pore volume have been observed with the incorporation of metal ions due to localized deposition of metals on the biochar surface and blockage of micropore entrance by magnesium oxide [47].

3.2.3. *Hydrophobicity, polarity, and aromaticity*

Studies have revealed that the CO_2 adsorption capacity of carbonaceous materials may be reduced under humid environments because of the high affinity for H_2O of most porous materials [90,91]. Biochar with hydrophobic and non-polar characteristics may facilitate the CO_2 adsorption capacity by limiting the competition of H_2O molecules. Low H/C and O/C ratios (<0.2), suggest a high degree of aromaticity and fixed carbon, which are chemically stable [65]. Very low O/C ratios have been found in white oak biochar ($O/C = 0.051$), and this is associated with high hydrophobicity, low polarity, and enhanced CO_2 capturing capacity of biochar [92]. Increasing pyrolysis temperature can separate H and O due to the fracture of chemical bonds. The molar ratio of O/C and H/C decreases as the increase of pyrolysis temperature (Table 1), possibly due to loss of volatile organic compounds and increase in dehydrogenation and deoxygenation reactions resulting formation of aromatic structures and reduce the polarity of biochar while increasing the hydrophobicity (Fig. 3) [31,60,77,93].

4. Modified biochar for CO_2 adsorption

Biochar has excellent inherent characteristics for capturing CO_2 because of its polar and hydrophilic nature with a highly porous structure and high specific surface area [18,48,95]. At present, scientists focus on the production of engineered/designer biochar through modification with novel structures to yield different surface properties and increase the sorption capacity [11,96]. The modification of biochar can be achieved through various methods, such as the use of different activation conditions, precursors, and additives [97,98]. The feedstock can be treated either prior to pyrolysis or after pyrolysis to achieve the desired changes to the biochar [94]. The modification of biochar can be categorized as chemical modification, physical modification, impregnation with elements, or grafting [99]. Table 2 summarizes the key findings of recent research on the use of modified biochar for CO_2 adsorption.

4.1. Alkali-modified biochar

The activation of biochar using KOH or NaOH dissolves ash and compounds like lignin and cellulose, which increases the O content and surface basicity of the biochar [100,101]. Two-stage KOH activation of pre-carbonized precursors may create a higher surface area with more surface hydroxyl groups than that of pristine biochar [102,103]. Moreover, during the KOH activation process, different potassium species, including K_2O and K_2CO_3, are formed and diffuse into the internal structure of the biochar matrix, which increases the width of the existing pores and generates new pores [104,105]. Nevertheless, the effect of alkali treatment on the formation of –OH in biochar depends on the type of feedstock, charring method, and treatment conditions, such as the activation temperature and ratio between alkali and C [6,31]. KOH-activated biochar has been found to yield a higher BET surface area ($1400\ m^2/g$) and higher ultra-micropore and super-micropore volume than those of CO_2- and steam-activated biochars leading to a significant increase in CO_2 adsorption capacity in KOH activated biochar than that of steam activated biochar (Table 2) [107]. KOH-activated biochar exhibits higher adsorption capacities than CO_2 and steam-activated biochar because of its higher surface area and micropore volume, irrespective of the presence of more oxygen-containing functional groups [5,107]. Moreover, Igalavithana et al. found that the development of micropores by KOH activation significantly increased the CO_2 adsorption [136].

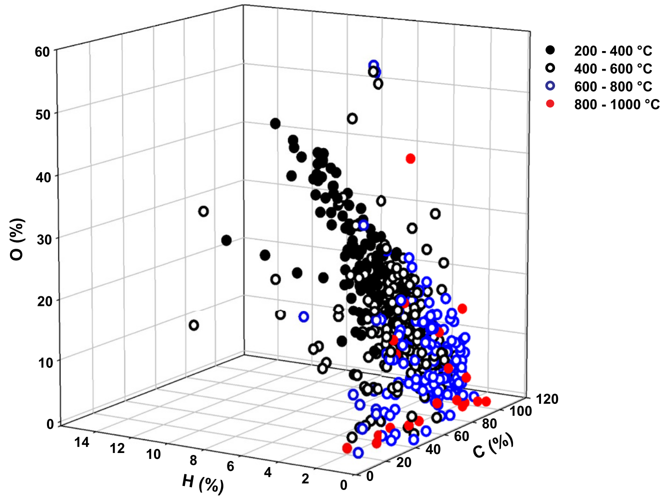

Fig. 3. Variation of carbon (C), hydrogen (H), and oxygen (O) (percentages) in biochar with the pyrolysis temperature (Adopted from Igalavithana et al. [94]).

4.2. Amino-modified biochar

Ammonia modification or the introduction of basic functional groups such as *N*-containing functional groups onto biochar surface increases the affinity of biochar for adsorbing acidic CO_2 as a result of the increase in alkalinity. Soybean straw biochar modified with CO_2–NH_3 had a higher CO_2 adsorption capacity (88.89 mg/g) than NH_3-modified (79.19 mg/g) and CO_2-modified (76.31 mg/g) biochar [67]. Contrasting results were observed in a study conducted with cotton stalk biochar produced by fast pyrolysis and modified with CO_2, NH_3, and $CO_2 + NH_3$ [57]. In that study, CO_2-modified biochar derived from cotton stalk at 800 °C performed better in CO_2 adsorption at 20 °C (99.42 mg/g) than the NH_3 or $NH_3 + CO_2$-modified biochars because of the better micropore structure [57]. However, the CO_2 adsorption capacity of biochar activated with either NH_3 or $NH_3 + CO_2$ increased with the increase of activation temperature from 500 °C to 800 °C where as a slight reduction in CO_2 adsorption could be observed in biochar activated with 900 °C compared to that of 800 °C (Table 2). A similar trend could be observed in the micropore surface area of biochar modified with NH_3 and $NH_3 + CO_2$. When biochar was modified first with CO_2 and followed by NH_3, CO_2 could combine with biochar surface to produce active sites to facilitate introducing N containing functional groups [66]. Nevertheless, introduction of excessive amounts of N functional groups may block the micropore entrance and reduce the surface area [66].

4.3. Carbon dioxide activation of biochar

Gas purging or the modification of biochar with CO_2 is a physical modification method [41,103,109]. Several studies have proven that CO_2 activation enhances micropores, which favors CO_2 adsorption [57,110]. During CO_2 modification, CO_2 reacts with the C of biochar to form CO (known as hot corrosion) and creates a more microporous structure [99]. Moreover, the gas purging facilitates the thermal degradation of carbonaceous material and enhances the aromaticity of the biochar [27,111]. Studies have revealed that the capacity of CO_2 adsorption in CO_2-modified biochar is significantly higher than that of unmodified biochar [41]. In addition, CO_2-modified biochar has a higher surface area and pore volume than unmodified and NH_3-modified biochar, and CO_2 adsorption capacity shows a significant linear relationship with the micropore volume [41,57]. Studies have revealed that the CO_2 adsorption capacity shows an increasing trend with increasing activation temperature (Table 2) [57]. In addition, after CO_2 activation, the synthesized carbon materials are of high purity, and, thus, a washing stage after completion of the activation process is not needed. Therefore, gas purging is more advantageous than chemical activation [112].

4.4. Steam-activated biochar

During steam activation, biochar is subjected to partial gasification with steam, which enhances the devolatilization and the formation of a crystalline structure [99]. The oxygen from water molecules in carbon

Table 2
Effect of biochar modification on its properties and CO_2 adsorption capacity.

Feedstock	Pyrolysis temperature (°C)	Modification method	BET surface area (m^2/g)	Surface area of micropores (m^2/g)	Total pore volume (cm^3/g)	Micropore volume (cm^3/g)	Adsorption temperature (°C)	CO_2 adsorption capacity (mg/g)	Reference
Whitewood	500	Steam activation	840	N/A	0.55	N/A	25	59	[107]
Whitewood	500	CO_2 activation	820	N/A	0.45	N/A	25	63	[107]
Whitewood	500	KOH activation	1400	N/A	0.62	N/A	25	78	[107]
Soybean straw	500	Raw biochar without activation	0.04	250	N/A	0.1	30	45 (Approx.)	[67]
Soybean straw	500	CO_2 activation at 500 °C	5.5	300	N/A	0.12	30	46 (Approx.)	[67]
Soybean straw	500	CO_2 activation at 600 °C	2.6	342	N/A	0.14	30	58 (Approx.)	[67]
Soybean straw	500	CO_2 activation at 700 °C	22	398	N/A	0.16	30	60 (Approx.)	[67]
Soybean straw	500	CO_2 activation at 800 °C	346	473	N/A	0.19	30	76 (Approx.)	[67]
Soybean straw	500	CO_2 activation at 900 °C	397	445	N/A	0.18	30	66 (Approx.)	[67]
Soybean straw	500	Ammonification with NH_3 at 500 °C	1.5	311	N/A	0.13	30	48 (Approx.)	[67]
Soybean straw	500	Ammonification with NH_3 at 600 °C	5.8	339	N/A	0.14	30	57 (Approx.)	[67]
Soybean straw	500	Ammonification with NH_3 at 700 °C	221	433	N/A	0.17	30	62 (Approx.)	[67]
Soybean straw	500	Ammonification with NH_3 at 800 °C	365	479	N/A	0.19	30	79 (Approx.)	[67]
Soybean straw	500	Ammonification with NH_3 at 900 °C	469	461	N/A	0.19	30	74 (Approx.)	[67]
Soybean straw	500	Treatment with CO_2–NH3 mixture at 500 °C	2	318	N/A	0.13	30	55 (Approx.)	[67]
Soybean straw	500	Treatment with CO_2–NH_3 mixture at 600 °C	1.2	370	N/A	0.15	30	60 (Approx.)	[67]
Soybean straw	500	Treatment with CO_2–NH_3 mixture at 700 °C	41	439	N/A	0.18	30	64 (Approx.)	[67]
Soybean straw	500	Treatment with CO_2–NH_3 mixture at 800 °C	491	534	N/A	0.21	30	89 (Approx.)	[67]
Soybean straw	500	Treatment with CO_2–NH_3 mixture at 900 °C	764	489	N/A	0.2	30	82 (Approx.)	[67]
Cotton stalk	600	Unmodified biochar	N/A	224	N/A	0.07	20	38 (Approx.)	[66]
Cotton stalk	600	Modified with CO_2 at 500 °C	N/A	289	N/A	0.12	20	53 (Approx.)	[66]
Cotton stalk	600	Modified with CO_2 at 600 °C	N/A	351	N/A	0.13	20	64 (Approx.)	[66]
Cotton stalk	600	Modified with CO_2 at 700 °C	N/A	372	N/A	0.14	20	66 (Approx.)	[66]
Cotton stalk	600	Modified with CO_2 at 800 °C	N/A	610	N/A	0.24	20	99.42	[66]
Cotton stalk		Modified with CO_2 at 900 °C	N/A	556	N/A	0.21	N/A	96 (Approx.)	[66]
Cotton stalk	600	Modified with NH_3 500 °C	N/A	161	N/A	0.06	N/A	26 (Approx.)	[66]
Cotton stalk	600	Modified with NH_3 600 °C	N/A	252	N/A	0.1	N/A	52 (Approx.)	[66]
Cotton stalk	600	Modified with NH_3 700 °C	N/A	255	N/A	0.1	N/A	50 (Approx.)	[66]
Cotton stalk	600	Modified with NH_3 800 °C	N/A	349	N/A	0.14	N/A	75 (Approx.)	[66]
Cotton stalk	600	Modified with NH_3 900 °C	N/A	435	N/A	0.17	N/A	78 (Approx.)	[66]
Cotton stalk	600	Modified with CO_2 and NH_3 mixture 500 °C	N/A	95	N/A	0.04	N/A	15 (Approx.)	[66]
Cotton stalk	600	Modified with CO_2 and NH_3 mixture 600 °C	N/A	297	N/A	0.12	120	52 (Approx.)	[66]
Cotton stalk	600	Modified with CO_2 and NH_3 mixture 700 °C	N/A	336	N/A	0.13	N/A	65 (Approx.)	[66]
Cotton stalk	600	Modified with CO_2 and NH_3 mixture 800 °C	N/A	627	N/A	0.25	N/A	95 (Approx.)	[66]
Cotton stalk	600	Modified with CO_2 and NH_3 mixture 900 °C	N/A	469	N/A	0.19	N/A	90 (Approx.)	[66]

(*continued on next page*)

Table 2 (*continued*)

Feedstock	Pyrolysis temperature (°C)	Modification method	BET surface area (m^2/g)	Surface area of micropores (m^2/g)	Total pore volume (cm^3/g)	Micropore volume (cm^3/g)	Adsorption temperature (°C)	CO_2 adsorption capacity (mg/g)	Reference
Cotton stalk	600	Unmodified biochar	224.12	N/A	N/A	0.07	20 120	58 (Approx.) 14 (Approx.)	[41]
Cotton stalk	600	Modified with NH_3 at 500 °C	N/A	160.89	N/A	0.06	20 120	46 (Approx.) 36 (Approx.)	[41]
Cotton stalk	600	Modified with NH_3 at 600 °C	N/A	251.91	N/A	0.08	20 120	50 (Approx.) 35 (Approx.)	[41]
Cotton stalk	600	Modified with NH_3 at 700 °C	N/A	254.97	N/A	0.14	20 120	60 (Approx.) 28 (Approx.)	[41]
Cotton stalk	600	Modified with NH_3 at 800 °C	N/A	348.56	N/A	0.17	20 120	72 (Approx.) 13 (Approx.)	[41]
Cotton stalk	600	Modified with NH_3 at 900 °C	N/A	434.92	N/A	0.19	20 120	78 (Approx.) 10 (Approx.)	[41]
Cotton stalk	600	Modified with CO_2 at 500 °C	N/A	289.07	N/A	0.12	20 120	64 (Approx.) 10 (Approx.)	[41]
Cotton stalk	600	Modified with CO_2 at 600 °C	N/A	351.49	N/A	0.13	20 120	54 (Approx.) 12 (Approx.)	[41]
Cotton stalk	600	Modified with CO_2 at 700 °C	N/A	371.65	N/A	0.14	20 120	72 (Approx.) 13 (Approx.)	[41]
Cotton stalk	800	Modified with CO_2 at 800 °C	N/A	610.04	N/A	0.24	20 120	96 (Approx.) 20 (Approx.)	[41]
Cotton stalk	600	Modified with CO_2 at 900 °C	N/A	556.35	N/A	0.21	20 120	80 (Approx.) 16 (Approx.)	[41]
Sawdust	450	Unmodified biochar	8.76	N/A	N/A	N/A	30	19.7	[43]
Sawdust	450	Unmodified biochar	8.76	N/A	N/A	N/A	70	13.5	[43]
Sawdust	450	Treatment with monoethanolamine	0.61	N/A	N/A	N/A	30	19.1	[43]
Sawdust	450	Treatment with monoethanolamine	0.61	N/A	N/A	N/A	70	12.1	[43]
Sawdust	450	Treatment with monoethanolamine	0.61	N/A	N/A	N/A	70	12.1	[43]
Sawdust	750	Unmodified biochar	1.36	N/A	N/A	N/A	30	45.2	[43]
Sawdust	750	Unmodified biochar	1.36	N/A	N/A	N/A	70	25.4	[43]
Sawdust	750	Treatment with monoethanolamine	0.15	N/A	N/A	N/A	30	39.7	[43]
Sawdust	750	Treatment with monoethanolamine	0.15	N/A	N/A	N/A	70	22.6	[43]
Sawdust	850	Unmodified biochar	182.04	N/A	N/A	N/A	30	47.5	[43]
Sawdust	850	Unmodified biochar	182.04	N/A	N/A	N/A	70	28.8	[43]
Sawdust	850	Treatment with monoethanolamine	3.17	N/A	N/A	N/A	30	44.8	[43]
Sawdust	850	Treatment with monoethanolamine	3.17	N/A	N/A	N/A	70	25.2	[43]
Walnut shell	500	Unmodified biochar	94.509	N/A	0.054	0.021	N/A	N/A	[47]
Walnut shell	900	Unmodified biochar	397.015	N/A	0.198	0.159	25 70	72.6 30.07	[47]
Walnut shell	900	Mg loaded	292.002	N/A	0.157	0.118	25 70	82.04 43.76	[47]
Cottonwood	600	Unmodified biochar (CW)	99	N/A	0.01	N/A	25	57.96	[108]
Cottonwood	600	Mg:CW = 0.01	275	N/A	0.01	N/A	25	63.69	[108]
Cottonwood	600	Mg:CW = 0.25	244	N/A	0.03	N/A	25	47.69	[108]
Cottonwood	600	Mg:CW = 1	184	N/A	0.1	N/A	25	35.35	[108]
Cottonwood	600	Mg:CW = 3	228	N/A	0.12	N/A	25	33.83	[108]
Cottonwood	600	Mg:CW = 6	197	N/A	0.29	N/A	25	27.79	[108]
Cottonwood	600	Mg:CW = 20	289	N/A	0.25	N/A	25	35.05	[108]
Cottonwood	600	Mg:CW = 40	262	N/A	0.27	N/A	25	32.33	[108]
Cottonwood	600	Al:CW = 0.025	256	N/A	0.01	N/A	25	63.87	[108]
Cottonwood	600	Al:CW = 0.25	206	N/A	0.03	N/A	25	62.98	[108]
Cottonwood	600	Al:CW = 2.5	331	N/A	0.3	N/A	25	69.3	[108]
Cottonwood	600	Al:CW = 1	263	N/A	0.25	N/A	25	64.63	[108]
Cottonwood	600	Al:CW = 3	370	N/A	0.39	N/A	25	69.49	[108]
Cottonwood	600	Al:CW = 4	367	N/A	0.37	N/A	25	71.05	[108]
Cottonwood	600	Fe:CW = 0.01	302	N/A	0.01	N/A	25	64.3	[108]
Cottonwood	600	Fe:CW = 0.05	NA	N/A	NA	N/A	25	55.61	[108]
Cottonwood	600	Fe:CW = 0.1	458	N/A	0.04	N/A	25	66.57	[108]
Cottonwood	600	Fe:CW = 5	665	N/A	0.59	N/A	25	60.68	[108]
Cottonwood	600	Fe:CW = 6	654	N/A	0.19	N/A	25	65.26	[108]
Cottonwood	600	Fe:CW = 10	749	N/A	0.33	N/A	25	53.79	[108]

surface sites, create surface oxides and H_2. Then, the produced H_2 reacts with C surface sites, forming surface hydrogen complexes and activating the biochar surface [99]. Even though CO_2-activated biochar and steam-activated biochar have similar micropore volumes, steam-activated biochar has a higher total pore volume than that of CO_2-activated biochar [107]. Steam-activated carbon has a higher graphitic carbon content and lower content of oxygen-containing functional groups than that of KOH-activated carbon [107]. However, it was found that the adsorption capacity of steam-activated carbon begins to reduce from the 20th cycle, which indicates that the steam-activated biochar may not be suitable for multicycle CO_2 adsorption [107].

4.5. Metal-impregnated biochar

Some studies have also used metal oxyhydroxide biochar composites to increase the adsorption capacity of biochar [49]. It has been found that the adsorption of acidic CO_2 can be enhanced by increasing the alkalinity of the biochar surface. Therefore, the introduction of metal groups including Na, Ca, Mg, Al, Ni, and Fe onto the biochar surface will increase basic sites on the surface of biochar, and hence, this method serves as a promising option to improve the CO_2 adsorption capacity of biochar [47]. Lahijani et al. [47] reported that a biochar incorporating Mg showed a higher CO_2 adsorption capacity (82.0 mg/g) than that of raw biochar (72.6 mg/g) at 25 °C and 1 atm (Table 2). Moreover, cyclic CO_2 capture studies showed that Mg-loaded biochar has high stability in its CO_2 capture capacity [47]. Generally, metal oxyhydroxides are basic and tend to bond with the CO_2 molecules which are acidic. Therefore, metal oxyhydroxide–biochar composites such as the Fe_2O_3–biochar composite, which has ferromagnetic properties because of the presence of iron oxide, can be used to enhance the CO_2 adsorption capacity of biochar [49]. Even though, the presence of larger surface area with abundant adsorption sites is important for high CO_2 adsorption, Creamer et al. [10] found a poor correlation between the surface area and CO_2 adsorption on biochar modified with aluminium oxide suggesting that presence of large surface area does not always ensure high adsorption. Moreover, interaction between iron oxide and CO_2 particles were significantly weaker than that of AlOOH [10].

5. Current challenges facing the practical application of biochar-based adsorbents

Biochar-based adsorbents have been claimed to have advantages of being low-cost, renewable, and suitable for the removal of multiple contaminants (i.e., they can remove chemical, biological, and physical contaminants), and, thus, they have been the subject of extensive studies over the past ten years [113]. However, there are still various challenges that prevent the practical, large-scale application of biochar-based adsorbents for CO_2 removal.

First, the robustness and stability of biochar-based adsorbents have not been fully demonstrated, despite the fact that high adsorption capacities and long-term cyclic operation are critical to ensure the economics and practicality of the technology [114]. Huang et al. [45] found that the CO_2 adsorption capacity of rice straw biochar produced by microwave pyrolysis was around 10 mg/g lower than that of activated carbon and suggested that processes such as activation and impregnation are required to enhance the capacity of the biochar. Lahijani et al. [47] impregnated walnut shell pyrolysis biochar with various types of metals (Mg, Al, Fe, Ni, Ca, and Na), followed by N_2 heat treatment, and found that the adsorption capacity increased from 72.6 mg/g for raw biochar to 82.0 mg/g for Mg-loaded biochar. Nevertheless, the enhanced adsorption is still significantly smaller than that of conventional activated carbon (e.g., type A-20, type Maxsorb III and phenol-formaldehyde resin-based), which has an adsorption capacity of several hundreds of milligrams per gram [115]. It is worth noting that any modification process may add extra costs and carbon footprint to the biochar-based adsorbents, and these have not been quantified yet.

Secondly, existing experiments are mainly based on simulated gas mixtures that consist of either pure CO_2 or a simple combination of several gas components (e.g., CO_2, N_2, and H_2O) [116]. For cases where multiple gaseous agents exist, it is important to know if the gases other than CO_2 will affect the adsorption capacity of CO_2 (i.e., competitive adsorption), as well as how the biochar affects the concentrations of these other gases. For example, the adsorption capacity of CO_2 could be reduced by the H_2O initially adsorbed on the carbon [116]. Few studies have investigated the use of biochar-based adsorbents to remove CO_2 in practical, large-scale applications [37]. The composition of actual flue or product gas can be more complicated than that of the simulated gas. Thus, more studies are required to clarify the principles and mechanisms underlying the competitive adsorption of biochar in actual flue or product gas so that specific biochar-based adsorbents can be developed for certain flue or product gas compositions. The CO_2 adsorption capacity of biochar in indoor spaces or a specific space can be predicted by airflow simulation programs using computational fluid dynamics (CFD). A 2D mathematical model for CO_2 absorption using CFD was developed by Hajilary and Rezakazemi [117], and, in their study, the simulation results were compared with the experimental data, and the effects of the liquid flow rate, different nanoparticles, and nanoparticle concentration on the process efficiency were investigated. Hooff and Blocken [118] conducted CFD simulation analysis on the natural ventilation of a large semi-enclosed stadium using the CO_2 concentration decay method.

Third, to complete the knowledge loop of the whole CO_2 capture and reuse cycle, it is also necessary to understand the principles and mechanisms for the regeneration and disposal of biochar. The regeneration ability for reuse of adsorbent after using for CO_2 removal is an important feature for determining the economic efficiency of the adsorbent [39]. Bamdad et al. [119] found that the CO_2 adsorption capacity of nitrogen-functionalized sawmill-residue-based biochar decreased by 4–8% after five cycles and by 20% after 10 cycles. Nguyen and Lee [39] showed that the CO_2 adsorption capacity of nitrogen doped biochar decreased by 15% after 10 cycles. Apart from that, metal oxy-hydroxide biochar composites produced using aluminium, iron or magnesium demonstrated excellent regeneration capacity ranging from 90 to 99% at 120 °C [108] which is relatively low regeneration temperature compared to other studies [120]. Activated carbon produced with KOH or CO_2 activation using biochar also exhibited good regeneration ability up to 50 cycles whereas adsorption capacity of steam activated carbon started to decrease after 20 cycles suggesting that steam activated carbon is not favorable for multi cyclic adsorption [107]. Although they claimed that the regeneration rates were satisfactory, higher rates have been achieved for other types of CO_2 adsorbents. For example, the CO_2 adsorption capacity of polyHIPE/PEI-based adsorbent only decreased by about 5% after 10 cycles [121], and the adsorption capacity of the APTES-grafted ordered mesoporous silica KIT-6 remained almost constant after 10 cycles [122]. The large loss in CO_2 capture capacity after cyclic adsorption may increase the cost of regeneration and limit the use of biochar as a carbon sequestering material. Alternatively, CO_2-saturated biochar can be used in an admixture to replace some of the cement used in building materials, which would lead to the valorization of biochar at the end of its service life as a CO_2 adsorbent. Gupta et al. [123] reported that the addition of 2% saw dust biochar saturated with CO_2 (SatBC) in cement mortar pre-deployment improved the early strength and reduced the water penetration depth compared to the control mortar. Although the 28-day strength and capillary absorption of SatBC was affected by the presence of CO_2 in the biochar pores, this type of biochar can be used in non-structural cement-based materials where strength and durability considerations are less important than those of structural materials [123].

Biochar may be contaminated by pollutants (e.g., Volatile Organic Compounds (VOCs), Polycyclic Aromatic Hydrocarbons (PAHs), heavy metals and particulates) during the production process and service life [12,65]. It has been found that PAHs concentration is greatly influenced by feedstock type and production temperature and resident time.

Biochar produced with slow pyrolysis possess low PAH content compared to that of fast pyrolysis possibly due to longer resident time during slow pyrolysis, PAHs may release to the gaseous phase whereas during fast pyrolysis or gasification, PAHs can be concentrated on biochar [124]. Buss et al. [125] found that PAH content in biochar produced from straw was 5.8 times higher than that of biochar produced with wood biomass suggesting that lignin content and the composition of lignin in biomass greatly influenced the PAH content in biochar. Apart from that, studies have observed that VOC content in biochar decreased with the increase of pyrolysing temperature and whereas gasification resulted in low levels of VOCs compared to hydrothermal carbonization [12]. Moreover, if the feedstock is naturally low in heavy metal content, biochar derived from that feedstock also consist of less amount of heavy metals suggesting that it is a prerequisite to select appropriate feedstock to ensure safe application [126]. Hence, careful selection of clean feedstock and appropriate conversion technology with proper temperature range and residence time is essential to minimize contaminants in biochar [12].

Kua et al. [127] studied the effect of particulate materials (0.27–22.50 μm) on the CO_2 adsorption capacity of biochar produced from wood waste at 500 °C and 10 °C/min. The study showed that the deposition of fine particulate material on the surfaces and pores of the biochar can reduce the CO_2 adsorption capacity by 8.33 times in an environment containing 600 ppm CO_2. However, limited information is available regarding the impact of chemical pollutants on the CO_2 adsorption capacity of biochar and the flue gas composition. The presence of the pollutants may indirectly affect the disposal of spent biochar, e.g., limiting its use as a soil additive [128,129]. Indeed, there is limited information regarding the ecotoxicology and human health risks associated with the use of biochar-based adsorbents [113]. Thus, it is necessary to develop specific standards about the concentrations of the pollutants in biochar for certain compositions of flue or product gas and for matching with the biochar disposal method.

Fourth, both physical and chemical modification methods have been proposed and tested in laboratory-scale experiments. However, most studies are explorative in nature and the effectiveness of the methods for large-scale biochar modification and application is still unclear. The techno-economic and environmental feasibility of the methods for the application of biochar-based adsorbents must be examined from a system and life-cycle perspective, as has been done for conventional carbon capture and sequestration technologies [130,131]]. For example, pyrolysis is an endothermic process and requires a sustained external heat source, whose impact on the whole-life-cycle carbon footprint of biochar-based CO_2 adsorption technology remains unclear. As far as possible, life-cycle assessments of biochar production and application systems should be consequential in nature so that the system boundaries (and, thus, the impacts assessed) include the co-products of the pyrolysis or gasification processes. Examples of consequential assessments for slag can be found in Kua et al. [133,134]. Correspondingly, the optimization and design parameters of practical, large-scale biochar-based CO_2 removal systems are still lacking. In addition, in terms of the indoor environment, it is possible to reduce the concentration of CO_2 in the indoor space by applying biochar to the filter of the ventilation device or the building materials. However, because the physical properties may change during the manufacture of building materials and filters including biochar, a clear test method for building materials must be reviewed. Such studies will shed light on how the price of biochar sorbents can be affected by various factors, such as labor, feedstock, production efficiencies [135], and even the pricing of the co-products.

Finally, it is desirable to develop a systematic database containing information ranging from the selection of suitable (cost, properties, or availability) feedstocks, physicochemical properties of biochar products, methods and effects of biochar upgrading, impacts of the presence of multiple gas agents, recovery of adsorbed CO_2, and regeneration and disposal of biochar, along with the relevant cost-benefit and environmental information. The database will serve as the basis for making an informed decision about the practical use of biochar-based adsorbents for CO_2 removal. The development of a databank of biochar-based adsorbents necessitates consistent or standardized experiment designs and data reporting, which do not currently exist.

6. Conclusions

Biochar is a potential cost-effective and sustainable material for CO_2 adsorption because of its inherent properties. However, the surface area, micropore area, micropore volume, presence of basic functional groups and hetero atoms play vital roles in the CO_2 adsorption capacity of biochar. Thus, the modification of biochar through chemical and physical processes to enhance the surface characteristics will significantly improve the CO_2 adsorption capacity of biochar. However, few studies have been performed with respect to the large-scale production and use of modified biochar for capturing CO_2. Hence, further studies should focus on the development of novel technologies and biochar composites such as metal organic framework (MOF) and carbon-based nanomaterials to enhance the CO_2 adsorption capacity of biochar. Moreover, the field-scale application of biochar for CO_2 adsorption should also be a focus in the future, as well as the development of new technologies for the regeneration and reuse of captured CO_2 or its conversion into useable products.

Acknowledgment

This study was supported by the Korea Ministry of Environment (MOE) as “Technology Program for establishing biocide safety management” (2018002490001) and Hydrogen Energy Innovation Technology Development Program of the National Research Foundation of Korea (NRF) funded by the Korean government (Ministry of Science and ICT(MSIT)) (NRF-2019M3E6A1064197).

References

[1] Liu C, Yao Z, Wang K, Zheng X, Li B. Net ecosystem carbon and greenhouse gas budgets in fiber and cereal cropping systems. Sci Total Environ 2019;647: 895–904. https://doi.org/10.1016/j.scitotenv.2018.08.048.

[2] Marescaux A, Thieu V, Garnier J. Carbon dioxide, methane and nitrous oxide emissions from the human-impacted Seine watershed in France. Sci Total Environ 2018;643:247–59. https://doi.org/10.1016/j.scitotenv.2018.06.151.

[3] IPCC. Climate change 2014: impacts, adaptation, and vulnerability. 2014. https://doi.org/10.1007/s13398-014-0173-7.2. Part B: Regional Aspects. Contribution of Working Group II to the Fifth Assessment Report of the Intergovernmental Panel on Climate Change [Barros, V.R., C.B. Field, D.J. Dokken, M.D pp. 688. IPCC, 2014: Climate Change 2014: Impacts, Adaptation, and Vulnerability. Part B: Regional Aspects. Contribution of Working Group II to the Fifth Assessment Report of the Intergovernmental Panel on Climate Change [Barros, V.R., C.B. Field, D.J. Dokken, M.D. Ipcc 2014:688.

[4] Dutcher B, Fan M, Russell AG. Amine-based CO_2 capture technology development from the beginning of 2013-A review. ACS Appl Mater Interfaces 2015;7: 2137–48. https://doi.org/10.1021/am507465f.

[5] Guo T, Ma N, Pan Y, Bedane AH, Xiao H, Eić M, et al. Characteristics of CO_2 adsorption on biochar derived from biomass pyrolysis in molten salt. Can J Chem Eng 2018;9999:1–9. https://doi.org/10.1002/cjce.23153.

[6] Zhao H, Luo X, Zhang H, Sun N, Wei W, Sun Y. Carbon-based adsorbents for post-combustion capture: a review. Greenhouse Gases Sci Technol 2018;8:11–36. https://doi.org/10.1002/ghg.1758.

[8] Yaumi AL, Bakar MZA, Hameed BH. Recent advances in functionalized composite solid materials for carbon dioxide capture. Energy 2017;124:461–80. https://doi.org/10.1016/j.energy.2017.02.053.

[9] Shafeeyan MS, Daud WMAW, Houshmand A, Shamiri A. A review on surface modification of activated carbon for carbon dioxide adsorption. J Anal Appl Pyrolysis 2010;89:143–51. https://doi.org/10.1016/j.jaap.2010.07.006.

[10] Creamer AE, Gao B. Carbon-based adsorbents for postcombustion CO_2 capture: a critical review. Environ Sci Technol 2016;50:7276–89. https://doi.org/10.1021/acs.est.6b00627.

[11] Shao J, Zhang J, Zhang X, Feng Y, Zhang H, Zhang S, et al. Enhance SO_2 adsorption performance of biochar modified by CO_2 activation and amine impregnation. Fuel 2018;224:138–46. https://doi.org/10.1016/j.fuel.2018.03.064.

[12] Ok YS, Tsang DC, Bolan N, Novak JM. Biochar from biomass and waste: fundamentals and applications. Elsevier; 2018, ISBN 9780128117309.

[13] Zhang X, Gao B, Creamer AE, Cao C, Li Y. Adsorption of VOCs onto engineered carbon materials: a review. J Hazard Mater 2017;338:102–23. https://doi.org/10.1016/j.jhazmat.2017.05.013.

[14] Liu WJ, Jiang H, Yu HQ. Development of biochar-based functional materials: toward a sustainable platform carbon material. Chem Rev 2015;115:12251–85. https://doi.org/10.1021/acs.chemrev.5b00195.

[15] El-Naggar A, Lee SS, Awad YM, Yang X, Ryu C, Rizwan M, et al. Influence of soil properties and feedstocks on biochar potential for carbon mineralization and improvement of infertile soils. Geoderma 2018;332:100–8. https://doi.org/10.1016/j.geoderma.2018.06.017.

[16] Ahmad M, Lee SS, Lee SE, Al-Wabel MI, Tsang DCW, Ok YS. Biochar-induced changes in soil properties affected immobilization/mobilization of metals/metalloids in contaminated soils. J Soils Sediments 2017;17:717–30. https://doi.org/10.1007/s11368-015-1339-4.

[17] Beiyuan J, Awad YM, Beckers F, Tsang DCW, Ok YS, Rinklebe J. Mobility and phytoavailability of as and Pb in a contaminated soil using pine sawdust biochar under systematic change of redox conditions. Chemosphere 2017;178:110–8. https://doi.org/10.1016/j.chemosphere.2017.03.022.

[18] Ahmad M, Rajapaksha AU, Lim JE, Zhang M, Bolan N, Mohan D, et al. Biochar as a sorbent for contaminant management in soil and water: a review. Chemosphere 2014;99:19–33. https://doi.org/10.1016/j.chemosphere.2013.10.071.

[19] Woolf D, Amonette JE, Street-Perrott FA, Lehmann J, Joseph S. Sustainable biochar to mitigate global climate change. Nat Commun 2010;1:1–9. https://doi.org/10.1038/ncomms1053.

[20] Xiong X, Yu IKM, Cao L, Tsang DCW, Zhang S, Ok YS. A review of biochar-based catalysts for chemical synthesis, biofuel production, and pollution control. Bioresour Technol 2017;246:254–70. https://doi.org/10.1016/j.biortech.2017.06.163.

[21] You S, Ok YS, Tsang DCW, Kwon EE, Wang H, You S, et al. Towards practical application of gasification : a critical review from syngas and biochar perspectives. Crit Rev Environ Sci Technol 2017;0:1–48. https://doi.org/10.1080/10643389.2018.1518860.

[22] Qian K, Kumar A, Zhang H, Bellmer D, Huhnke R. Recent advances in utilization of biochar. Renew Sustain Energy Rev 2015;42:1055–64. https://doi.org/10.1016/j.rser.2014.10.074.

[23] Inyang MI, Gao B, Yao Y, Xue Y, Zimmerman A, Mosa A, et al. Technology A review of biochar as a low-cost adsorbent for aqueous heavy metal removal. Crit Rev Environ Sci Technol 2016;46:406–33. https://doi.org/10.1080/10643389.2015.1096880.

[24] Rajapaksha AU, Ok YS, El-Naggar A, Kim H, Song F, Kang S, et al. Dissolved organic matter characterization of biochars produced from different feedstock materials. J Environ Manag 2019;233:393–9. https://doi.org/10.1016/j.jenvman.2018.12.069.

[25] He X, Liu Z, Niu W, Yang L, Zhou T, Qin D, et al. Effects of pyrolysis temperature on the physicochemical properties of gas and biochar obtained from pyrolysis of crop residues. Energy 2018;143:746–56. https://doi.org/10.1016/j.energy.2017.11.062.

[26] Yang X, Yu IKM, Cho D-W, Chen SS, Tsang DCW, Shang J, et al. Tin-functionalized wood biochar as a sustainable solid catalyst for glucose isomerization in biorefinery. ACS Sustainable Chem Eng 2019;7. https://doi.org/10.1021/acssuschemeng.8b05311. acssuschemeng.8b05311.

[27] Yang X, Tsibart A, Nam H, Hur J, El-Naggar A, Tack FMG, et al. Effect of gasification biochar application on soil quality: trace metal behavior, microbial community, and soil dissolved organic matter. J Hazard Mater 2019;365:684–94. https://doi.org/10.1016/j.jhazmat.2018.11.042.

[28] Ashiq A, Adassooriya NM, Sarkar B, Rajapaksha AU, Ok YS, Vithanage M. Municipal solid waste biochar-bentonite composite for the removal of antibiotic ciprofloxacin from aqueous media. J Environ Manag 2019;236:428–35. https://doi.org/10.1016/j.jenvman.2019.02.006.

[29] Melo TM, Bottlinger M, Schulz E, Leandro WM, Menezes de Aguiar Filho A, Wang H, et al. Plant and soil responses to hydrothermally converted sewage sludge (sewchar). Chemosphere 2018;206:338–48. https://doi.org/10.1016/j.chemosphere.2018.04.178.

[30] Li Y, Ruan G, Jalilov AS, Tarkunde YR, Fei H, Tour JM. Biochar as a renewable source for high-performance CO_2 sorbent. Carbon N Y 2016;107:344–51. https://doi.org/10.1016/j.carbon.2016.06.010.

[31] Huang H, Tang J, Gao K, He R, Zhao H, Werner D. Characterization of KOH modified biochars from different pyrolysis temperatures and enhanced adsorption of antibiotics. RSC Adv 2017;7:14640–8. https://doi.org/10.1039/c6ra27881g.

[32] Sophia AC, Lima EC. Removal of emerging contaminants from the environment by adsorption. Ecotoxicol Environ Saf 2018;150:1–17. https://doi.org/10.1016/j.ecoenv.2017.12.026.

[33] Xu X, Schierz A, Xu N, Cao X. Comparison of the characteristics and mechanisms of Hg(II) sorption by biochars and activated carbon. J Colloid Interface Sci 2016;463:55–60. https://doi.org/10.1016/j.jcis.2015.10.003.

[34] Alhashimi HA, Aktas CB. Life cycle environmental and economic performance of biochar compared with activated carbon: a meta-analysis. Resour Conserv Recycl 2017;118:13–26.

[35] Lehmann J, Roberts KG, Gloy BA, Joseph S, Scott NR. Life cycle assessment of biochar systems: estimating the energetic, economic, and climate change potential. Environ Sci Technol 2010;44:827–33. https://doi.org/10.1021/es902266r.

[36] Rajapaksha AU, Chen SS, Tsang DCW, Zhang M, Vithanage M, Mandal S, et al. Engineered/designer biochar for contaminant removal/immobilization from soil and water: potential and implication of biochar modification. Chemosphere 2016;148:276–91. https://doi.org/10.1016/j.chemosphere.2016.01.043.

[37] Wang B, Gao B, Fang J. Recent advances in engineered biochar productions and applications. Crit Rev Environ Sci Technol 2017;47:2158–207. https://doi.org/10.1080/10643389.2017.1418580.

[38] Chatterjee R, Sajjadi B, Mattern DL, Chen WY, Zubatiuk T, Leszczynska D, et al. Ultrasound cavitation intensified amine functionalization: a feasible strategy for enhancing CO_2 capture capacity of biochar. Fuel 2018;225:287–98. https://doi.org/10.1016/j.fuel.2018.03.145.

[39] Nguyen MV, Lee BK. A novel removal of CO_2 using nitrogen doped biochar beads as a green adsorbent. Process Saf Environ Prot 2016;104:490–8. https://doi.org/10.1016/j.psep.2016.04.007.

[40] Zhang X, Zhang S, Yang H, Feng Y, Chen Y, Wang X, et al. Nitrogen enriched biochar modified by high temperature CO_2-ammonia treatment: characterization and adsorption of CO_2. Chem Eng J 2014;257:20–7. https://doi.org/10.1016/j.cej.2014.07.024.

[41] Xiong Z, Shihong Z, Haiping Y, Tao S, Yingquan C, Hanping C. Influence of NH_3/CO_2 modification on the characteristic of biochar and the CO_2 capture. Bioenergy Res 2013;6:1147–53. https://doi.org/10.1007/s12155-013-9304-9.

[42] Azlina W, Ab W, Ghani K, Rebitanim NZ, Amran M, Salleh M, et al. Carbon dioxide adsorption on coconut shell. Biochar 2015;1:683–93. https://doi.org/10.1007/978-3-319-16709-1.

[43] Madzaki H, Karimghani WAWAB. Nurzalikharebitanim, azilbaharialias. Carbon dioxide adsorption on sawdust biochar. Procedia Eng 2016;148:718–25. https://doi.org/10.1016/j.proeng.2016.06.591.

[44] Liu SH, Huang YY. Valorization of coffee grounds to biochar-derived adsorbents for CO_2 adsorption. J Clean Prod 2018;175:354–60. https://doi.org/10.1016/j.jclepro.2017.12.076.

[45] Huang YF, Chiueh PT, Shih CH, Lo SL, Sun L, Zhong Y, et al. Microwave pyrolysis of rice straw to produce biochar as an adsorbent for CO_2 capture. Energy 2015;84:75–82. https://doi.org/10.1016/j.energy.2015.02.026.

[46] Xu X, Kan Y, Zhao L, Cao X. Chemical transformation of CO_2 during its capture by waste biomass derived biochars. Environ Pollut 2016;213:533–40. https://doi.org/10.1016/j.envpol.2016.03.013.

[47] Lahijani P, Mohammadi M, Mohamed AR. Metal incorporated biochar as a potential adsorbent for high capacity CO_2 capture at ambient condition. J CO2 Util 2018;26:281–93. https://doi.org/10.1016/j.jcou.2018.05.018.

[48] Creamer AE, Gao B, Zhang M. Carbon dioxide capture using biochar produced from sugarcane bagasse and hickory wood. Chem Eng J 2014;249:174–9. https://doi.org/10.1016/j.cej.2014.03.105.

[49] Creamer AE, Gao B, Wang S. Carbon dioxide capture using various metal oxyhydroxide-biochar composites. Chem Eng J 2016;283:826–32. https://doi.org/10.1016/j.cej.2015.08.037.

[50] Plaza MG, González AS, Pis JJ, Rubiera F, Pevida C. Production of microporous biochars by single-step oxidation: effect of activation conditions on CO_2 capture. Appl Energy 2014;114:551–62. https://doi.org/10.1016/j.apenergy.2013.09.058.

[51] Sethupathi S, Zhang M, Rajapaksha AU, Lee SR, Nor NM, Mohamed AR, et al. Biochars as potential adsorbers of CH_4, CO_2 and H_2S. Sustain Times 2017;9:1–10. https://doi.org/10.3390/su9010121.

[52] Plaza MG, García S, Rubiera F, Pis JJ, Pevida C. Post-combustion CO_2 capture with a commercial activated carbon: comparison of different regeneration strategies. Chem Eng J 2010;163:41-47.doi.org/10.1016/j.cej.2010.07.030.

[53] Gargiulo V, Gomis-Berenguer A, Giudicianni P, Ania CO, Ragucci R, Alfe M. Assessing the potential of bio-chars prepared by steam assisted slow pyrolysis for CO_2 adsorption and separation. Energy Fuels 2018. https://doi.org/10.1021/acs.energyfuels.8b01058.

[54] Chiang Y, Juang R. Journal of the Taiwan Institute of Chemical Engineers Surface modifications of carbonaceous materials for carbon dioxide adsorption : a review. J Taiwan Inst Chem Eng 2017;71:214–34. https://doi.org/10.1016/j.jtice.2016.12.014.

[55] Liu Y, Lonappan L, Brar SK, Yang S. Impact of biochar amendment in agricultural soils on the sorption, desorption, and degradation of pesticides: a review. Sci Total Environ 2018;645:60–70. https://doi.org/10.1016/j.scitotenv.2018.07.099.

[56] Sun Y, Gao B, Yao Y, Fang J, Zhang M, Zhou Y, et al. Effects of feedstock type, production method, and pyrolysis temperature on biochar and hydrochar properties. Chem Eng J 2014;240:574–8. https://doi.org/10.1016/j.cej.2013.10.081.

[57] Zhang X, Zhang S, Yang H, Feng Y, Chen Y, Wang X, et al. Nitrogen enriched biochar modified by high temperature CO_2-ammonia treatment: characterization and adsorption of CO_2. Chem Eng J 2014;257:20–7. https://doi.org/10.1016/j.cej.2014.07.024.

[58] Igalavithana AD, Lee SE, Lee YH, Tsang DCW, Rinklebe J, Kwon EE, et al. Heavy metal immobilization and microbial community abundance by vegetable waste and pine cone biochar of agricultural soils. Chemosphere 2017;174:593–603. https://doi.org/10.1016/j.chemosphere.2017.01.148.

[59] Kim KH, Kim JY, Cho TS, Choi JW. Influence of pyrolysis temperature on physicochemical properties of biochar obtained from the fast pyrolysis of pitch pine (Pinus rigida). Bioresour Technol 2012;118:158–62. https://doi.org/10.1016/j.biortech.2012.04.094.

[60] Shaaban A, Se SM, Dimin MF, Juoi JM, Mohd Husin MH, Mitan NMM. Influence of heating temperature and holding time on biochars derived from rubber wood sawdust via slow pyrolysis. J Anal Appl Pyrolysis 2014;107:31–9. https://doi.org/10.1016/j.jaap.2014.01.021.

[61] Gai X, Wang H, Liu J, Zhai L, Liu S, Ren T, et al. Effects of feedstock and pyrolysis temperature on biochar adsorption of ammonium and nitrate. PLoS One 2014;9:1–19. https://doi.org/10.1371/journal.pone.0113888.

[62] Ng WC, You S, Ling R, Gin KYH, Dai Y, Wang CH. Co-gasification of woody biomass and chicken manure: syngas production, biochar reutilization, and cost-benefit analysis. Energy 2017;139:732–42. https://doi.org/10.1016/j.energy.2017.07.165.

[63] Zhang J, Huang B, Chen L, Li Y, Li W, Luo Z. Characteristics of biochar produced from yak manure at different pyrolysis temperatures and its effects on the yield and growth of highland barley. Chem Speciat Bioavailab 2018;00:1–11. https://doi.org/10.1080/09542299.2018.1487774.

[64] Liu Y, Yao S, Wang Y, Lu H, Brar SK, Yang S. Bio- and hydrochars from rice straw and pig manure: inter-comparison. Bioresour Technol 2017;235:332–7. https://doi.org/10.1016/j.biortech.2017.03.103.

[65] You S, Ok YS, Chen SS, Tsang DCW, Kwon EE, Lee J, et al. A critical review on sustainable biochar system through gasification: energy and environmental applications. Bioresour Technol 2017;246:242–53. https://doi.org/10.1016/j.biortech.2017.06.177.

[66] Zhang X, Zhang S, Yang H, Feng Y, Chen Y, Wang X, et al. Nitrogen enriched biochar modified by high temperature CO_2-ammonia treatment: characterization and adsorption of CO_2. Chem Eng J 2014;257:20–7. https://doi.org/10.1016/j.cej.2014.07.024.

[67] Zhang X, Wu J, Yang H, Shao J, Wang X, Chen Y, et al. Preparation of nitrogen-doped microporous modified biochar by high temperature CO_2-NH_3 treatment for CO_2 adsorption: effects of temperature. RSC Adv 2016;6:98157–66. https://doi.org/10.1039/c6ra23748g.

[68] Palansooriya KN, Wong JTF, Hashimoto Y, Huang L, Rinklebe J, Chang SX, et al. Response of microbial communities to biochar-amended soils: a critical review. Biochar 2019;1:3–22. https://doi.org/10.1007/s42773-019-00009-2.

[69] Hansen V, Müller-Stöver D, Ahrenfeldt J, Holm JK, Henriksen UB, Hauggaard-Nielsen H. Gasification biochar as a valuable by-product for carbon sequestration and soil amendment. Biomass Bioenergy 2015;72:300–8. https://doi.org/10.1016/j.biombioe.2014.10.013.

[70] Chen B, Zhou D, Zhu L. Transitional adsorption and partition of nonpolar and polar aromatic contaminants by biochars of pine needles with different pyrolytic temperatures. Environ Sci Technol 2008;42:5137–43. https://doi.org/10.1021/es8002684.

[71] Yang X, Igalavithana AD, Oh SE, Nam H, Zhang M, Wang CH, et al. Characterization of bioenergy biochar and its utilization for metal/metalloid immobilization in contaminated soil. Sci Total Environ 2018;640–641:704–13. https://doi.org/10.1016/j.scitotenv.2018.05.298.

[72] Mayakaduwa SS, Herath I, Ok YS, Mohan D, Vithanage M. Insights into aqueous carbofuran removal by modified and non-modified rice husk biochars. Environ Sci Pollut Res 2017;24:22755–63. https://doi.org/10.1007/s11356-016-7430-6.

[73] Sun Y, Gao B, Yao Y, Fang J, Zhang M, Zhou Y, et al. Effects of feedstock type, production method, and pyrolysis temperature on biochar and hydrochar properties. Chem Eng J 2014;240:574–8. https://doi.org/10.1016/j.cej.2013.10.081.

[74] Sigmund G, Bucheli TD, Hilber I, Micić V, Kah M, Hofmann T. Effect of ageing on the properties and polycyclic aromatic hydrocarbon composition of biochar. Environ Sci Process Impacts 2017;19:768–74. https://doi.org/10.1039/c7em00116a.

[75] Wang S, Gao B, Zimmerman AR, Li Y, Ma L, Harris WG, et al. Physicochemical and sorptive properties of biochars derived from woody and herbaceous biomass. Chemosphere 2015;134:257–62. https://doi.org/10.1016/j.chemosphere.2015.04.062.

[76] Cao X, Harris W. Properties of dairy-manure-derived biochar pertinent to its potential use in remediation. Bioresour Technol 2010;101:5222–8. https://doi.org/10.1016/j.biortech.2010.02.052.

[77] Cantrell KB, Hunt PG, Uchimiya M, Novak JM, Ro KS. Impact of pyrolysis temperature and manure source on physicochemical characteristics of biochar. Bioresour Technol 2012;107:419–28. https://doi.org/10.1016/j.biortech.2011.11.084.

[78] Lee J, Yang X, Cho SH, Kim JK, Lee SS, Tsang DCW, et al. Pyrolysis process of agricultural waste using CO_2 for waste management, energy recovery, and biochar fabrication. Appl Energy 2017;185:214–22. https://doi.org/10.1016/j.apenergy.2016.10.092.

[79] Pacioni TR, Soares D, Domenico M Di, Rosa MF, Moreira R de FPM, José HJ. Bio-syngas production from agro-industrial biomass residues by steam gasification. Waste Manag 2016;58:221–9. https://doi.org/10.1016/j.wasman.2016.08.021.

[80] Zhang Z, Zhou J, Xing W, Xue Q, Yan Z, Zhuo S, et al. Critical role of small micropores in high CO_2 uptake. Phys Chem Chem Phys 2013;15:2523. https://doi.org/10.1039/c2cp44436d.

[81] Sevilla M, Fuertes AB. CO_2 adsorption by activated templated carbons. J Colloid Interface Sci 2012;366:147–54. https://doi.org/10.1016/j.jcis.2011.09.038.

[82] Chiang YC, Juang RS. Surface modifications of carbonaceous materials for carbon dioxide adsorption: a review. J Taiwan Inst Chem Eng 2017;71:214–34. https://doi.org/10.1016/j.jtice.2016.12.014.

[83] Angin D. Effect of pyrolysis temperature and heating rate on biochar obtained from pyrolysis of safflower seed press cake. Bioresour Technol 2013;128:593–7. https://doi.org/10.1016/j.biortech.2012.10.150.

[84] Zhang Z, Zhou J, Xing W, Xue Q, Yan Z, Zhuo S, et al. Critical role of small micropores in high CO_2 uptake. Phys Chem Chem Phys 2013;15:2523. https://doi.org/10.1039/c2cp44436d.

[85] Shafeeyan MS, Daud WMAW, Houshmand A, Shamiri A. A review on surface modification of activated carbon for carbon dioxide adsorption. J Anal Appl Pyrolysis 2010;89:143–51. https://doi.org/10.1016/j.jaap.2010.07.006.

[86] Shen W, Fan W. Nitrogen-containing porous carbons: synthesis and application. J Mater Chem 2013;1:999–1013. https://doi.org/10.1039/c2ta00028h.

[87] Xing W, Liu C, Zhou Z, Zhou J, Wang G, Zhuo S, et al. Oxygen-containing functional group-facilitated CO_2 capture by carbide-derived carbons. Nanoscale Res Lett 2014;9:1–8. https://doi.org/10.1186/1556-276X-9-189.

[88] Liu Y, Wilcox J. Effects of surface heterogeneity on the adsorption of CO_2 in microporous carbons. Environ Sci Technol 2012;46:1940–7. https://doi.org/10.1021/es204071g.

[89] Shahkarami S, Dalai AK, Soltan J. Enhanced CO_2 adsorption using MgO-impregnated activated carbon: impact of preparation techniques. Ind Eng Chem Res 2016;55:5955–64. https://doi.org/10.1021/acs.iecr.5b04824.

[90] Nugent P, Giannopoulou EG, Burd SD, Elemento O, Giannopoulou EG, Forrest K, et al. Porous materials with optimal adsorption thermodynamics and kinetics for CO_2 separation. Nature 2013;495:80–4. https://doi.org/10.1038/nature11893.

[91] Gao F, Li Y, Bian Z, Hu J, Liu H. Dynamic hydrophobic hindrance effect of zeolite@zeolitic imidazolate framework composites for CO_2 capture in the presence of water. J Mater Chem 2015;3:8091–7. https://doi.org/10.1039/c4ta06645f.

[92] Shen Y, Linville JL, Ignacio-de Leon PAA, Schoene RP, Urgun-Demirtas M. Towards a sustainable paradigm of waste-to-energy process: enhanced anaerobic digestion of sludge with woody biochar. J Clean Prod 2016;135:1054–64. https://doi.org/10.1016/j.jclepro.2016.06.144.

[93] Keiluweit M, Nico PS, Johnson MG. Dynamic molecular structure of plant biomass-derived black carbon (biochar). Environ Sci Technol 2010;44:1247–53.

[94] Igalavithana AD, Mandal S, Niazi NK, Vithanage M, Parikh SJ, Mukome FND, et al. Advances and future directions of biochar characterization methods and applications. Crit Rev Environ Sci Technol 2017;47:2275–330. https://doi.org/10.1080/10643389.2017.1421844.

[95] Regmi P, Garcia Moscoso JL, Kumar S, Cao X, Mao J, Schafran G. Removal of copper and cadmium from aqueous solution using switchgrass biochar produced via hydrothermal carbonization process. J Environ Manag 2012;109:61–9. https://doi.org/10.1016/j.jenvman.2012.04.047.

[96] Ok YS, Chang SX, Gao B, Chung HJ. SMART biochar technology-A shifting paradigm towards advanced materials and healthcare research. Environ Technol Innov 2015;4:206–9. https://doi.org/10.1016/j.eti.2015.08.003.

[97] Igalavithana AD, Mandal S, Niazi NK, Vithanage M, Parikh SJ, Mukome FND, et al. Advances and future directions of biochar characterization methods and applications. Crit Rev Environ Sci Technol 2017;47:2275–330. https://doi.org/10.1080/10643389.2017.1421844.

[98] Yao Y, Gao B, Fang J, Zhang M, Chen H, Zhou Y, et al. Characterization and environmental applications of clay-biochar composites. Chem Eng J 2014;242:136–43. https://doi.org/10.1016/j.cej.2013.12.062.

[99] Upamali A, Chen SS, Tsang DCW, Zhang M, Vithanage M, Mandal S, et al. Chemosphere Engineered/designer biochar for contaminant removal/immobilization from soil and water : potential and implication of biochar modification. Chemosphere 2016;148:276–91. https://doi.org/10.1016/j.chemosphere.2016.01.043.

[100] Fan Y, Wang B, Yuan S, Wu X, Chen J, Wang L. Adsorptive removal of chloramphenicol from wastewater by NaOH modified bamboo charcoal. Bioresour Technol 2010;101:7661–4. https://doi.org/10.1016/j.biortech.2010.04.046.

[101] Li J, Lv G, Bai W, Liu Q, Zhang Y, Song J. Modification and use of biochar from wheat straw (*Triticum aestivum* L.) for nitrate and phosphate removal from water. Desalin Water Treat 2014;57:1–13. https://doi.org/10.1080/19443994.2014.994104.

[102] Basta AH, Fierro V, El-Saied H, Celzard A. 2-Steps KOH activation of rice straw: an efficient method for preparing high-performance activated carbons. Bioresour Technol 2009;100:3941–7. https://doi.org/10.1016/j.biortech.2009.02.028.

[103] Bhatnagar A, Hogland W, Marques M, Sillanpää M. An overview of the modification methods of activated carbon for its water treatment applications. Chem Eng J 2013;219:499–511. https://doi.org/10.1016/j.cej.2012.12.038.

[104] Otowa T, Nojima Y, Miyazaki T. Development of KOH activated high surface area carbon and its application to drinking water purification. Carbon N Y 1997;35:1315–9. https://doi.org/10.1016/S0008-6223(97)00076-6.

[105] Mao H, Zhou D, Hashisho Z, Wang S, Chen H, Wang H. Preparation of pinewood- and wheat straw-based activated carbon via a microwave-assisted potassium hydroxide treatment and an analysis of the effects of the microwave activation conditions. BioResources 2015;10:809–21. https://doi.org/10.15376/biores.10.1.809-821.

[107] Shahkarami S, Azargohar R, Dalai AK, Soltan J. Breakthrough CO_2 adsorption in bio-based activated carbons. J Environ Sci (China) 2015;34:68–76. https://doi.org/10.1016/j.jes.2015.03.008.

[108] Creamer AE, Gao B, Wang S. Carbon dioxide capture using various metal oxyhydroxide – biochar composites. Chem Eng J 2016;283:826–32. https://doi.org/10.1016/j.cej.2015.08.037.

[109] Guo S, Peng J, Li W, Yang K, Zhang L, Zhang S, et al. Effects of CO_2 activation on porous structures of coconut shell-based activated carbons. Appl Surf Sci 2009;255:8443–9. https://doi.org/10.1016/j.apsusc.2009.05.150.

[110] Rashidi NA, Yusup S. An overview of activated carbons utilization for the post-combustion carbon dioxide capture. J CO2 Util 2016;13:1–16. https://doi.org/10.1016/j.jcou.2015.11.002.

[111] Igalavithana AD, Yang X, Zahra HR, Tack FMG, Tsang DCW, Kwon EE, et al. Metal (loid) immobilization in soils with biochars pyrolyzed in N_2 and CO_2 environments. Sci Total Environ 2018;630:1103–14. https://doi.org/10.1016/j.scitotenv.2018.02.185.

[112] Rashidi NA, Yusup S. An overview of activated carbons utilization for the post-combustion carbon dioxide capture. Biochem Pharmacol 2016;13:1–16. https://doi.org/10.1016/j.jcou.2015.11.002.

[113] Gwenzi W, Chaukura N, Noubactep C, Mukome FND. Biochar-based water treatment systems as a potential low-cost and sustainable technology for clean water provision. J Environ Manag 2017;197:732–49. https://doi.org/10.1016/j.jenvman.2017.03.087.

[114] Han Y, Cao X, Ouyang X, Sohi SP, Chen J. Adsorption kinetics of magnetic biochar derived from peanut hull on removal of Cr (VI) from aqueous solution: effects of production conditions and particle size. Chemosphere 2016;145:336–41. https://doi.org/10.1016/j.chemosphere.2015.11.050.

[115] Singh VK, Anil Kumar E. Measurement and analysis of adsorption isotherms of CO_2 on activated carbon. Appl Therm Eng 2016;97:77–86. https://doi.org/10.1016/j.applthermaleng.2015.10.052.

[116] Plaza MG, Durán I, Querejeta N, Rubiera F, Pevida C. Experimental and simulation study of adsorption in postcombustion conditions using a microporous biochar. 1. CO_2 and N_2 adsorption. Ind Eng Chem Res 2016;55:3097–112. https://doi.org/10.1021/acs.iecr.5b04856.

[117] Hajilary N, Rezakazemi M. CFD modeling of CO_2 capture by water-based nanofluids using hollow fiber membrane contactor. Int J Greenh Gas Control 2018;77:88–95. https://doi.org/10.1016/j.ijggc.2018.08.002.

[118] Van Hooff T, Blocken B. CFD evaluation of natural ventilation of indoor environments by the concentration decay method: CO_2 gas dispersion from a semi-enclosed stadium. Build Environ 2013;61:1–17. https://doi.org/10.1016/j.buildenv.2012.11.021.

[119] Bamdad H, Hawboldt K, MacQuarrie S. Nitrogen functionalized biochar as a renewable adsorbent for efficient CO_2 removal. Energy Fuels 2018;32:11742–8. https://doi.org/10.1021/acs.energyfuels.8b03056.

[120] Ghanbari S, Kamath G. Dynamic simulation and mass transfer study of carbon dioxide capture using biochar and MgO impregnated activated carbon in a swing adsorption process. Energy Fuels 2019;33. https://doi.org/10.1021/acs.energyfuels.9b00923. acs.energyfuels.9b00923.

[121] Irani M, Jacobson AT, Gasem KAM, Fan M. Facilely synthesized porous polymer as support of poly(ethyleneimine) for effective CO_2 capture. Energy 2018;157:1–9. https://doi.org/10.1016/j.energy.2018.05.141.

[122] Kishor R, Ghoshal AK. APTES grafted ordered mesoporous silica KIT-6 for CO_2 adsorption. Chem Eng J 2015;262:882–90. https://doi.org/10.1016/j.cej.2014.10.039.

[123] Gupta S, Kua HW, Low CY. Use of biochar as carbon sequestering additive in cement mortar. Cement Concr Compos 2018;87:110–29. https://doi.org/10.1016/j.cemconcomp.2017.12.009.

[124] Hilber I, Mayer P, Gouliarmou V, Hale SE, Cornelissen G, Schmidt HP, et al. Bioavailability and bioaccessibility of polycyclic aromatic hydrocarbons from (post-pyrolytically treated) biochars. Chemosphere 2017;174:700–7. https://doi.org/10.1016/j.chemosphere.2017.02.014.

[125] Buss W, Graham MC, MacKinnon G, Mašek O. Strategies for producing biochars with minimum PAH contamination. J Anal Appl Pyrolysis 2016;119:24–30. https://doi.org/10.1016/j.jaap.2016.04.001.

[126] Yang X, Ng W, Wong BSE, Baeg GH, Wang CH, Ok YS. Characterization and ecotoxicological investigation of biochar produced via slow pyrolysis: effect of feedstock composition and pyrolysis conditions. J Hazard Mater 2019;365:178–85. https://doi.org/10.1016/j.jhazmat.2018.10.047.

[127] Kua H, Pedapati C, Lee R. Production SK-J of C, 2018 undefined. Effect of indoor contamination on carbon dioxide adsorption of wood-based biochar–lessons for direct air capture, 210. Elsevier; 2019. p. 860–71. https://doi.org/10.1016/j.jclepro.2018.10.206.

[128] Dutta T, Kwon E, Bhattacharya SS, Jeon BH, Deep A, Uchimiya M, et al. Polycyclic aromatic hydrocarbons and volatile organic compounds in biochar and biochar-amended soil: a review. GCB Bioenergy 2017;9:990–1004. https://doi.org/10.1111/gcbb.12363.

[129] Hilber I, Bastos AC, Loureiro S, Soja G, Marsz A, Cornelissen G, et al. The different faces of biochar: contamination risk versus remediation tool. J Environ Eng Landsc Manag 2017;25:86–104. https://doi.org/10.3846/16486897.2016.1254089.

[130] Parker L, Folger P, Stine DD. Capturing CO from coal-fired power plants: challenges for a comprehensive strategy. CRS Rep Congr. 2008.

[131] Smebye AB, Sparrevik M, Schmidt HP, Cornelissen G. Life-cycle assessment of biochar production systems in tropical rural areas: comparing flame curtain kilns to other production methods. Biomass Bioenergy 2017;101:35–43. https://doi.org/10.1016/j.biombioe.2017.04.001.

[133] Kua HW. Integrated policies to promote sustainable use of steel slag for construction - a consequential life cycle embodied energy and greenhouse gas emission perspective. Energy Build 2015;101:133–43. https://doi.org/10.1016/j.enbuild.2015.04.036.

[134] Kua HW. The consequences of substituting sand with used copper slag in construction: an embodied energy and global warming potential analysis using life cycle approach and different allocation methods kua life cycle assessment of copper slag. J Ind Ecol 2013;17:869–79. https://doi.org/10.1111/jiec.12059.

[135] Gupta S, Wei H, Dai S. Biochar-mortar composite : manufacturing, evaluation of physical properties and economic viability. Constr Build Mater 2018;167:874–89. https://doi.org/10.1016/j.conbuildmat.2018.02.104.

[136] Igalavithana AD, Choi SW, Disssanayake PD, Shang J, Wang C-H, Yang X, et al. Gasification biochar from biowaste (food waste and wood waste) for effective CO_2 adsorption. J. Hazard Mater. 2019. https://doi.org/10.1016/j.jhazmat.2019.121147.